Dynamic Analysis and Control Design of Kinematically-Driven Multibody Mechanical Systems

Carmine Maria Pappalardo, Domenico Guida

Abstract—**In this investigation, a method for solving the dynamics and control problems of multibody mechanical systems whose time evolution is induced by a kinematically-driven motion is presented. In particular, the motion of a double inverted pendulum is employed as a demonstrative example of the computational procedure developed in this work and the interaction between the pantograph and the catenary is considered as a case study. To this end, the dynamic analysis and the design of a control system are performed. The multibody approach is used for deriving a mechanical model of the double inverted pendulum as well as of the pantograph mechanism. The multibody mechanical model developed in this work is aimed at improving the interaction force between the catenary and the pantograph. The mathematical method devised in this work for constructing multibody models of constrained mechanical systems makes use of a recursive Lagrangian approach. The Lagrangian formulation used in this paper allows for effectively handling the redundancy of the generalized coordinates and leads to a straightforward determination of the nonlinear reaction force fields arising from the presence of the mechanical joints. While the pantograph mechanism is schematized as a multibody mechanism having a geometrically nonlinear structure, the interaction force between the pan-head and the suspended line is modeled in a simplified manner considering a linear elastic element. On the other hand, a force actuator is applied between the upper arm and the pan-head of the pantograph mechanism for controlling the coupled dynamics of the pantagraph system and the catenary cable. The control system is devised with a twofold objective, namely to attenuate the interaction forces generated by the pantograph/catenary contact and to reduce the nonlinear oscillations of the closed-loop mechanism. An optimal law for the control action is obtained by employing a numerical algorithm based on the adjoint method. The numerical results found by means of numerical experiments demonstrate the efficacy of the recursive Lagrangian approach proposed in this work.**

Index Terms—**Recursive Lagrangian formulation, Multibody system dynamics, Kinematically-driven mechanical systems, Nonlinear optimal control, Double inverted pendulum, Pantograph mechanism.**

I. Introduction

This investigation is focused on the dynamic modeling of kinematically-driven multibody mechanical systems in order to be able to design nonlinear controllers for the contact forces generated between the pantograph and the catenary. To this end, the analytical methodology developed in this paper is first applied to the dynamic analysis of a double inverted pendulum used as a demonstrative example. Subsequently, an open-loop control architecture is considered and a rigid multibody model of the pantograph mechanism is employed for the synthesis of a control law developed using the optimal control theory. In this introductive section, background information, the significance of this research work, the synopsis of the issues addressed in this paper, a brief literature review, the contributions and the scope of this investigation, and the organization of the manuscript are presented.

C. M. Pappalardo is with the *Department of Industrial Engineering, University of Salerno*, Via Giovanni Paolo II, 132, 84084 Fisciano, Salerno, ITALY (corresponding author, email: cpappalardo@unisa.it).

D. Guida is with with the *Department of Industrial Engineering, University of Salerno*, Via Giovanni Paolo II, 132, 84084 Fisciano, Salerno, ITALY (email: guida@unisa.it).

A. Background Information and Significance of the Research

In recent years, computer simulations of mechanical systems have become pervasive in all engineering fields. Dynamic simulations allow for performing complex numerical experiments with a relatively simple mathematical model of a dynamical system for gaining insights into the system properties that are of interest to a particular engineering application [1]–[3]. To this end, the virtual prototyping of complex mechanical systems based on computer simulations leads to a low-cost estimation of the approximate dynamic behavior of alternative concepts based on simple mathematical models [4]–[6]. By doing so, the engineering design process based on computer simulations allows for the optimization of the performance of the final design. Furthermore, once that a mathematical model of a physical system has been verified experimentally, validated dynamic simulations can also be used for monitoring, diagnostics, and failure prediction of real prototypes [7]–[9]. For example, computer simulations based on the analytical approach developed for multibody mechanical systems represent an important tool for the transient analysis of vehicle systems, structural elements, aerospace applications, robots, and biomechanical devices [10]–[12].

B. Formulation of the Problem of Interest

The pantograph/catenary system is the main energy collection mechanism used in railway applications. The stability of this current collection system is particularly important when the electrical trains move at a high velocity [13]–[15]. In this dynamic problem, the contact force between the pantograph and the catenary is one of the most important factors that determine the correct operational state of electric trains. Consequently, the magnitude and the variation of the nonlinear force generated by the interaction between these mechanical components must be carefully regulated taking into account the dynamic behavior of this complex mechanical system. Furthermore, the fluctuation of the interaction force must be

properly predicted and controlled without affecting its average value in order to avoid the deterioration of the suspended infrastructure or a possible loss of power of traction due to the lack of contact. A viable solution for this issue is the application of a control actuator between the pantograph upper arm and the pan-head [16], [17]. This design solution has a significant potential for improving the performance of the quality of the contact of the mechanical components subjected to continuous wear. For example, an open-loop control policy and/or a state feedback control strategy could be used to design an appropriate control system [18]–[20]. Therefore, this solution is explored in this investigation. From a computational viewpoint, a pantograph/catenary model can be obtained using a multibody approach. In the literature, one can find various different studies focused on several practical issues related to the pantograph mechanism and the suspended electrical line. In many cases, the dynamics, control, and identification methods used in conjunction with the approach that is of interest for this research work are employed [21]–[24]. This fact is an indication of the importance of the issue addressed in this paper. On the other hand, as discussed in detail throughout the manuscript, an analytical strategy based on a recursive Lagrangian approach is adopted in this investigation for modeling the pantograph/catenary system considering an augmented formulation [25]–[27].

C. Literature Review

Multibody dynamics is an interdisciplinary field of research concentrated on the analysis and the synthesis of the motion of mechanical systems constrained by kinematic pairs [28], [29]. From a general perspective, multibody systems are mechanical systems composed of fundamental objects such as rigid bodies, flexible bodies, kinematic joints, force fields, force elements, control actuators, and motion sensors [30], [31]. Several examples of machines and mechanisms modeled as multibody systems are present in the literature [32]. The complex time evolution of a multibody system is governed by differential-algebraic equations (DAEs) associated with the system motion that are capable of capturing the inherent nonlinear dynamic nature of this class of dynamical systems [33], [34]. Therefore, appropriate dynamic solution procedures are necessary for obtaining reliable computer simulations of the dynamics of interest described by robust, stable, and consistent results. As mentioned before, rigid multibody systems are constituted of mechanical components interconnected between each other. An important aspect that characterizes the motion of rigid multibody systems is the presence of high nonlinearities which represent an intrinsic property of the system geometry [35]. This challenging issue is addressed in this study employing the combination of the augmented formulation for computing the generalized acceleration vector of the multibody equations of motion with the adjoint approach for the optimal determination of appropriate nonlinear control laws.

The dynamic study of the transient and steady-state behavior of the pantograph mechanism represents an important issue of modern mechanical engineering. In the literature, there are different research works focused on multiple engineering problems related to the pantograph/catenary system. Song et al. employed a nonlinear finite element procedure and the sliding mode control strategy for modeling and controlling the pantograph/catenary interaction under a stochastic wind field [36], [37]. Ko et al. devised a robust feedback controller for the pantograph/catenary system based on a linear optimal control algorithm and a sliding mode observer [38]. Zhang et al. used the numerical methods of computational fluid dynamics for evaluating the aerodynamic performances of high-speed trains considering the pantograph fixed in different configurations [39]. Li et al. analyzed the scenario in which the train passes through a gallery and analyzed the influence of the velocity of the train on the aerodynamic forces exerted on the pantograph structure as well as on the resulting interaction with the catenary [40]. Navik et al. investigated possible solutions for the assessment of the transient behavior of the railway catenary system based on sampled measurements using the modal analysis [41], [42]. Schirrer et al. set up a test rig for the pantograph mechanism with an accurate emulation of the catenary system that allows for performing several test campaigns and implemented an advanced impedance control for matching the desired dynamic behavior of the catenary wire [43], [44]. Zhang et al. employed a hybrid simulation procedure for the static and dynamic modeling of the pantograph mechanism and the catenary system introducing a mixed theoretical-experimental technique [45], [46]. Daocharoenporn et al. employed computational multibody system algorithms for developing detailed railroad vehicle models to estimate the wear resulting from the pantograph/catenary dynamic interaction [47]. Lu et al. proposed two estimator-based H-infinite control strategies to decrease the contact force fluctuation of the pantograph/catenary system considering the actuator time delay [48]. Vesali et al. studied the quality contact between the pantograph and the catenary system and proposed a method for increasing the velocity of electric trains [49]. Zdziebko et al. investigated the use of active control strategies applied to a railway pantograph in order to improve contact quality in the pantograph/catenary interface [50]. The abundant number of investigations concentrated on the study of the coupled behavior of the pantograph mechanism and the catenary system is an indication of the importance of the problem addressed in this paper [51], [52].

D. Scope and Contributions

In this work, two kinematically-driven multibody mechanical systems are analyzed, namely a double inverted pendulum system and a pantograph/catenary system. The former system is used in the paper as a demonstrative example, while the latter system represents the main object of this investigation. In particular, the set of nonlinear DAEs that model the pantograph/catenary system is obtained considering a multibody approach which includes the constraint equations representing the closed-chain structure of the pantograph mechanism. Subsequently, a nonlinear control law based on a feedforward architecture is derived for improving the quality of the contact between the pantograph mechanism and the suspended catenary. To this end, a method relying on an adjoint-based computational approach is employed. The adjoint-based method used in the paper performs an iterative optimization of the open-loop control action generated by the nonlinear dynamic behavior of the pantograph/catenary

system. In order to prove the efficacy of the approach devised in the paper, a nonlinear dynamic analysis is carried out. Numerical experiments demonstrate that the application of the optimal controller devised in the paper by using the adjoint approach can considerably improve the contact performance.

The multibody modeling approach employed in the paper mathematically represents the pantograph as a closed-chain planar linkage having the same kinematic structure of a four-bar mechanism composed only of rigid bodies. A nonlinear pneumatic actuator is considered for modeling the lifting force exerted on the pantograph mechanism. The pneumatic actuator is modeled as a lumped parameter component characterized by a nonlinear elastic element combined with a linear damping element. In a similar manner, the pantograph suspension system is schematized considering linear elastic and viscous elements. The nonlinear contact force resulting from the interaction between the pantograph mechanism and the suspended catenary cable is modeled as elastic support which excites the pantograph pan-head with a prescribed motion law. The external motion of the moving support models the dynamic interaction between the pantograph pan-head and the catenary cable considering the superposition of two harmonic functions representing respectively the geometry of the span of the suspended line and the effect of the distance between the droppers that connects the suspended cables. The nonlinear influence of both these dynamic effects is considered in the transient analysis of the pantograph mechanism.

In this paper, the dynamic model of the double inverted pendulum is derived by using a recursive Lagrangian approach, while the dynamic equations of the pantograph/catenary system are first obtained without considering the constraint equations arising from the closed-chain topology of this multibody mechanism. Subsequently, the closed-loop constraint equations associated with the kinematic structure of the multibody system at hand are enforced using a multibody technique based on the augmented formulation. This method relies on the Lagrangian formulation approach to analytical dynamics. In particular, the augmented formulation approach is constructed using a set of redundant generalized coordinates. Furthermore, this method allows for computing the generalized constraint forces of a general multibody mechanical system having a three-dimensional configuration restricted by kinematic pairs. On the other hand, a controlled force based on a pure feedforward control scheme is used in the paper for ameliorating the contact performance. The nonlinear open-loop control force is designed using a general iterative procedure based on the adjoint method. The adjoint method is a computational method that allows for solving in an effective and efficient way complex nonlinear optimization problems such as the differential-algebraic two-point boundary value problem that originates from the application of the optimal control theory to nonlinear dynamical systems. The adjoint-based computational procedure carries out an iterative optimization of the control actions for nonlinear dynamical systems. The numerical algorithm based on the adjoint method combines a nonlinear conjugate gradient procedure with a numerical strategy for effectively evaluating the gradient of the cost functional. The computational steps of the control optimization scheme associated with the adjoint method are reported in the paper.

In this investigation, a nonlinear controller based on a feedforward architecture and acting between the pantograph mechanism and the catenary system is developed. The goal of the control law is twofold, namely to attenuate the mechanical oscillations of the pantograph mechanism and, at the same time, to reduce the attrition of the pantograph components. Several dynamical simulations are performed in the paper in order to demonstrate that the optimal control action computed employing the adjoint method significantly improves the contact performance of the pantograph multibody system and the suspended catenary cable.

E. Paper Organization

This paper is written considering the following structure. In Section II, the differential-algebraic equations of motion of a general multibody system are recalled and the adjoint method for the optimal design of nonlinear control laws is discussed. In Section III, the dynamic analysis of a kinematically-driven double inverted pendulum is presented and is used as a demonstrative example of the computational approach developed in the paper. In Section IV, the key features of the pantograph mechanism that represents the case study of interest for this work are described and the numerical results found using the recursive multibody approach employed in the paper are illustrated. In Section V, a summary of the manuscript and the conclusions found in this work are provided.

II. Analytical Methods and Computational Algorithms

In this section, the formulation of the equations of motion in the standard descriptor form of a general multibody system and the adjoint method for optimal control are discussed. To this end, the mathematical background for the kinematic, dynamic, and control analysis of multibody mechanical systems formed by rigid components is briefly recalled. The principal equations necessary for modeling rigid multibody mechanical systems in a two-dimensional space are described considering an analytical formulation approach based on the planar Reference Point Coordinate Formulation (RPCF) with Euler Angles (EA) [53]. In particular, a new analytical formulation for the derivation of the equations of motion of kinematically-driven mechanical systems is proposed in this section. Subsequently, the fundamental aspects necessary for implementing the optimization of nonlinear control actions are provided for the benefit of the reader that may be unfamiliar with the theory of nonlinear optimal control. Finally, a new computational procedure based on the adjoint method suitable for solving the resulting differential-algebraic two-point boundary value problem associated with the optimal determination of nonlinear control laws is described herein.

A. Equations of Motion of Kinematically-Driven Rigid Multibody Systems

In this subsection, the differential-algebraic dynamic equations of a general multibody system are presented. Thereafter, the mathematical background necessary for the kinematic description and the dynamic analysis of multibody systems

composed only of rigid bodies is discussed. For this purpose, the differential-algebraic dynamic equations of rigid multibody systems are formally derived employing the Lagrange equations of the first kind, which represents one of the fundamental principles of classical mechanics, in conjunction with the Lagrange multipliers technique [54], [55]. The resulting set of equations of motion forms a highly nonlinear system of Differential-Algebraic Equations (DAEs) and requires the use of numerical techniques for obtaining an approximate solution.

The study of the kinematics of a multibody system constituted by rigid bodies in two-dimensional or three-dimensional spaces represents a crucial aspect for the correct development of the differential-algebraic equations of motion [56]. In particular, a fundamental aspect of the kinematic analysis of a rigid multibody system is represented by the understanding of the motion of the different bodies and components that form the system itself [57]. When the multibody system of interest consists only of rigid components, the kinematics of a body belonging to the system is completely described by the kinematics of a frame coordinate system which is rigidly connected to a point of the rigid body. This frame of reference is formed by three orthogonal axes and it is referred to as the floating frame of reference system. Therefore, the local position of a particle on a body of the rigid system under consideration can be described by means of the fixed components along the axes of this moving coordinates system. In particular, Chasles' theorem of classical mechanics states that, in general, the displacement of a frame of reference collocated on a rigid body can be described by the combination of a translation and a rotation about an instantaneous axis of rotation. Hence, it is of paramount importance to understand the mathematical description of the rotation in the space to properly describe the general motion of a rigid multibody system. The basic mathematical equation that serves to this purpose is called the fundamental formula of rigid kinematics and is given by:

$$\mathbf{r}_b(P) = \mathbf{R} + \mathbf{A}\bar{\mathbf{u}}(P) = \mathbf{R} + \mathbf{u}(P) \tag{1}$$

where $\mathbf{r}_b(P)$ denotes the global position of the material point P attached to the rigid body, $\mathbf{R} = \mathbf{r}_b(O)$ identifies the global position of the origin O of the reference frame collocated on the rigid body, $\bar{\mathbf{u}}(P)$ represents the local position of the material point P, and $\mathbf{A}$ is the rotation matrix that transforms vector quantities defined in the body-fixed reference system, like the local position vector $\bar{\mathbf{u}}(P)$, into the equivalent vector quantities defined in the global frame of reference, like the global position vector $\mathbf{u}(P) = \mathbf{A}\bar{\mathbf{u}}(P)$. The fundamental equations of rigid kinematics allow for defining the position field of the rigid body using a set of translational and rotational generalized coordinates that appear in the position vector $\mathbf{R}$ and in the rotation matrix $\mathbf{A}$. Starting from the position field $\mathbf{r}_b(P)$, which is defined in a two-dimensional space or in a three-dimensional space, one can directly obtain the velocity field $\mathbf{v}_b(P) = \dot{\mathbf{r}}_b(P)$ and the acceleration field $\mathbf{a}_b(P) = \dot{\mathbf{v}}_b(P) = \ddot{\mathbf{r}}_b(P)$ of the rigid body by computing the first and second time derivatives of the position field as follows:

$$\begin{cases} \mathbf{v}_b(P) = \dot{\mathbf{r}}_b(P) = \dot{\mathbf{R}} + \boldsymbol{\omega} \times \mathbf{u}(P) \\ \mathbf{a}_b(P) = \dot{\mathbf{v}}_b(P) = \ddot{\mathbf{r}}_b(P) \\ \qquad = \ddot{\mathbf{R}} + \dot{\boldsymbol{\omega}} \times \mathbf{u}(P) + \boldsymbol{\omega} \times [\boldsymbol{\omega} \times \mathbf{u}(P)] \end{cases} \tag{2}$$

where t represents the time independent variable, $\boldsymbol{\omega}$ is the angular velocity vector of the rigid body, while $\dot{\mathbf{R}} = d\mathbf{R}/dt$, $\ddot{\mathbf{R}} = d\dot{\mathbf{R}}/dt = d^2\mathbf{R}/dt^2$, and $\dot{\boldsymbol{\omega}} = d\boldsymbol{\omega}/dt$ are respectively total time derivatives of the body-fixed global position vector and of the angular velocity vector. Furthermore, it can be easily proved that the velocity and acceleration fields of the rigid body can be equivalently expressed by using vector quantities defined in the body-fixed frame of reference as follows:

$$\begin{cases} \mathbf{v}_b(P) = \dot{\mathbf{R}} + \mathbf{A}\left[\bar{\boldsymbol{\omega}} \times \bar{\mathbf{u}}(P)\right] \\ \mathbf{a}_b(P) = \ddot{\mathbf{R}} + \mathbf{A}\left[\dot{\bar{\boldsymbol{\omega}}} \times \bar{\mathbf{u}}(P)\right] \\ \qquad + \mathbf{A}\left\{\bar{\boldsymbol{\omega}} \times [\bar{\boldsymbol{\omega}} \times \bar{\mathbf{u}}(P)]\right\} \end{cases} \tag{3}$$

where $\bar{\boldsymbol{\omega}}$ represents the projection on the local reference frame of the body angular velocity vector and $\dot{\bar{\boldsymbol{\omega}}} = d\bar{\boldsymbol{\omega}}/dt$. This second formulation is mathematically equivalent to the first formalism but is more convenient to use when one needs to describe the kinematics of complex mechanisms such as the double inverted pendulum system and the pantograph system considered in this research work.

When one wants to obtain the dynamic equations of a kinematically-driven mechanical system, for example, the double inverted pendulum that is driven by the motion of the cart or the pantograph mechanism driven by the motion of the catenary cable considered in this research work, the following recursive analytical procedure can be used. Immediately after the kinematic description discussed before, the subsequent fundamental step of the dynamic analysis is to explicitly determine the linear velocity vector and the angular velocity vector of the frame of reference pertaining to each rigid body that forms the mechanical system. To this end, one can write:

$$\dot{\mathbf{R}} = \mathbf{J}\dot{\mathbf{q}} + \mathbf{v}, \quad \boldsymbol{\omega} = \boldsymbol{\Omega}\dot{\mathbf{q}} + \mathbf{w} \tag{4}$$

where $\mathbf{q}$ denotes the system configuration vector, $\dot{\mathbf{q}} = d\mathbf{q}/dt$ represents the system generalized velocity vector, $\mathbf{v}$ and $\mathbf{w}$ are known vector functions of time, while $\mathbf{J} = \partial\mathbf{R}/\partial\mathbf{q}$ and $\boldsymbol{\Omega} = \partial\boldsymbol{\omega}/\partial\dot{\mathbf{q}}$ are Jacobian matrices that are respectively associated with the linear velocity field and the angular velocity field of the rigid body. Considering a frame of reference attached to the center of mass G of the rigid body under consideration, one can express the total kinetic energy T of the body as follows:

$$\begin{aligned} T &= \tfrac{1}{2}\int_V \rho v_b^2(P)dV = \tfrac{1}{2}\int_V \rho \mathbf{v}_b^T(P)\mathbf{v}_b(P)dV \\ &= \tfrac{1}{2}\int_V \rho \dot{\mathbf{r}}_b^T(P)\dot{\mathbf{r}}_b(P)dV = T_q + T_l + T_c \end{aligned} \tag{5}$$

where V is the volume of the rigid body, ρ identifies the body mass density, T_q denotes the quadratic part of the total kinetic energy, T_l represents the linear part of the total kinetic

energy, and T_c identifies the scalar part of the total kinetic energy which are respectively defined as:

$$T_q = \frac{1}{2}\dot{\mathbf{q}}^T\mathbf{M}\dot{\mathbf{q}}, \quad T_l = \frac{1}{2}\mathbf{b}^T\dot{\mathbf{q}}, \quad T_c = \frac{1}{2}c \tag{6}$$

where $\mathbf{M}$ indicates the mass matrix of the rigid body, $\mathbf{b}$ is a multiplicative vector associated with the linear part of the kinetic energy, and c is an additional scalar term that are respectively given by:

$$\mathbf{M} = m\mathbf{J}^T\mathbf{J} + \mathbf{\Omega}^T\mathbf{I}_G\mathbf{\Omega}, \quad \mathbf{b} = 2m\mathbf{J}^T\mathbf{v} + 2\mathbf{\Omega}^T\mathbf{I}_G\mathbf{w} \tag{7}$$

and

$$c = m\mathbf{v}^T\mathbf{v} + \mathbf{w}^T\mathbf{I}_G\mathbf{w} \tag{8}$$

where m indicates the mass of the rigid body and $\mathbf{I}_G$ corresponds to the body inertia matrix referred to the body-fixed reference system with origin in the center of mass G. For the explicit derivation of the dynamic terms that appear in the equations of motion, it is convenient to use the following definition of the kinetic energy induced by the kinematically-driven motion T_m:

$$\begin{aligned} T_m &= T_l + T_c = \tfrac{1}{2}\mathbf{b}^T\dot{\mathbf{q}} + \tfrac{1}{2}c \\ &= m\mathbf{v}^T\mathbf{J}\dot{\mathbf{q}} + \mathbf{w}^T\mathbf{I}_G\mathbf{\Omega}\dot{\mathbf{q}} + \tfrac{1}{2}m\mathbf{v}^T\mathbf{v} + \tfrac{1}{2}\mathbf{w}^T\mathbf{I}_G\mathbf{w} \end{aligned} \tag{9}$$

At this stage, the Lagrange equations of the first kind can be invoked and used for computing the vector and matrix quantities necessary for describing the nonlinear dynamics of the mechanical system of interest. For this purpose, one can write:

$$\frac{d}{dt}\left(\frac{\partial T}{\partial \dot{\mathbf{q}}}\right)^T - \left(\frac{\partial T}{\partial \mathbf{q}}\right)^T + \left(\frac{\partial \mathbf{C}}{\partial \mathbf{q}}\right)^T\boldsymbol{\lambda} = \mathbf{Q}_e \tag{10}$$

where $\mathbf{C}$ is a nonlinear vector of algebraic equations that model the kinematic joints, $\boldsymbol{\lambda}$ identifies the Lagrange multiplier vector, and the nonlinear vector $\mathbf{Q}_e$ contains the total external generalized forces applied on the mechanical system. By manipulating the Lagrange equations of the first kind, one obtains the following analytical forms:

$$\mathbf{Q}_v = \left(\frac{\partial T_q}{\partial \mathbf{q}}\right)^T - \dot{\mathbf{M}}\dot{\mathbf{q}} \tag{11}$$

and

$$\mathbf{Q}_m = \left(\frac{\partial T_m}{\partial \mathbf{q}}\right)^T - \frac{d}{dt}\left(\frac{\partial T_m}{\partial \dot{\mathbf{q}}}\right)^T \tag{12}$$

where $\mathbf{Q}_v$ is the vector that absorbs the inertial terms that are quadratic in the generalized velocities and $\mathbf{Q}_m$ is the kinematically-driven generalized force vector applied to the mechanical system.

Employing the Lagrange equations of the first kind as a primary principle of the analytical dynamics, consider the following formalism for the differential-algebraic dynamic equations of a multibody mechanical system formed by rigid bodies and kinematic pairs:

$$\begin{cases} \mathbf{M}\ddot{\mathbf{q}} = \mathbf{Q}_v + \mathbf{Q}_m + \mathbf{Q}_e - \mathbf{C}_\mathbf{q}^T\boldsymbol{\lambda} \\ \\ \mathbf{C}_\mathbf{q}\ddot{\mathbf{q}} = \mathbf{Q}_d \end{cases} \tag{13}$$

where $\ddot{\mathbf{q}} = d\dot{\mathbf{q}}/dt = d^2\mathbf{q}/dt^2$ identifies the system generalized acceleration vector, $\mathbf{M}$ corresponds to the system mass matrix, $\mathbf{Q}_v$ is the total inertia quadratic velocity vector of the rigid bodies, $\mathbf{Q}_m$ indicates a nonlinear vector of generalized forces associated with the kinematically-driven components of the mechanical system, $\mathbf{Q}_e$ represents the total generalized external force vector acting on the rigid bodies, $\mathbf{C}_\mathbf{q} = \partial\mathbf{C}/\partial\mathbf{q}$ corresponds to the constraint Jacobian matrix, and $\mathbf{Q}_d$ is the quadratic velocity vector associated with the algebraic constraints. This nonlinear set of DAEs can be readily rewritten in the following matrix form which is referred to as the augmented formulation:

$$\begin{bmatrix} \mathbf{M} & \mathbf{C}_\mathbf{q}^T \\ \mathbf{C}_\mathbf{q} & \mathbf{O} \end{bmatrix}\begin{bmatrix} \ddot{\mathbf{q}} \\ \boldsymbol{\lambda} \end{bmatrix} = \begin{bmatrix} \mathbf{Q}_b \\ \mathbf{Q}_d \end{bmatrix} \tag{14}$$

where the total vector of generalized forces applied to the rigid body is indicated with $\mathbf{Q}_b$ and is given by:

$$\mathbf{Q}_b = \mathbf{Q}_v + \mathbf{Q}_m + \mathbf{Q}_e \tag{15}$$

By solving the previous system of linear equations at each time step of the dynamical simulation, the generalized acceleration vector $\ddot{\mathbf{q}}$ and the Lagrange multiplier vector $\boldsymbol{\lambda}$ of the multibody system can be explicitly calculated as:

$$\begin{cases} \ddot{\mathbf{q}} = \mathbf{M}^{-1}\mathbf{Q}_b \\ \quad +\mathbf{M}^{-1}\mathbf{C}_\mathbf{q}^T\left(\mathbf{C}_\mathbf{q}\mathbf{M}^{-1}\mathbf{C}_\mathbf{q}^T\right)^{-1}\mathbf{Q}_d \\ \quad -\mathbf{M}^{-1}\mathbf{C}_\mathbf{q}^T\left(\mathbf{C}_\mathbf{q}\mathbf{M}^{-1}\mathbf{C}_\mathbf{q}^T\right)^{-1}\mathbf{C}_\mathbf{q}\mathbf{M}^{-1}\mathbf{Q}_b \\ \\ \boldsymbol{\lambda} = -\left(\mathbf{C}_\mathbf{q}\mathbf{M}^{-1}\mathbf{C}_\mathbf{q}^T\right)^{-1}\left(\mathbf{Q}_d - \mathbf{C}_\mathbf{q}\mathbf{M}^{-1}\mathbf{Q}_b\right) \end{cases} \tag{16}$$

The Lagrange multiplier vector $\boldsymbol{\lambda}$ can be used for calculating the generalized force vector relative to the kinematic constraints acting on the mechanical system $\mathbf{Q}_c$ as follows:

$$\mathbf{Q}_c = -\mathbf{C}_\mathbf{q}^T\boldsymbol{\lambda} \tag{17}$$

On the other hand, the generalized acceleration vector $\ddot{\mathbf{q}}$ of the mechanical systems can be employed for the progressive marching of the numerical simulation on the time grid using a standard numerical integration technique.

B. Numerical Solution of the Equations of Motion

In this subsection, the solution algorithms suitable for solving the equations of motion of kinematically-driven multibody systems are briefly discussed. In order to perform dynamical simulations of nonlinear systems, the following simple definition of the state vector can be used:

$$\mathbf{z} = \begin{bmatrix} \mathbf{q} \\ \dot{\mathbf{q}} \end{bmatrix} \tag{18}$$

The mathematical formulation of the state vector $\mathbf{z}$ is necessary for writing the nonlinear set of the system dynamic equations in the state-space form as follows:

$$\dot{\mathbf{z}} = \mathbf{f} \tag{19}$$

where the nonlinear vector function $\mathbf{f}$ identifies the system state function and is defined as:

$$\mathbf{f} = \begin{bmatrix} \dot{\mathbf{q}} \\ \ddot{\mathbf{q}} \end{bmatrix} \tag{20}$$

The general state-space representation of the dynamic equations of a rigid multibody system allows for using the numerical integration procedure developed for solving system of Ordinary Differential Equations (ODEs) in order

to obtain an approximate solution of the dynamic equations. For example, one can obtain a numerical solution of the dynamic equations of a multibody system by using the first-order explicit Euler method given by:

$$\mathbf{Z}^{n+1} = \mathbf{Z}^n + \Delta t \mathbf{f}(t^n, \mathbf{Z}^n) \tag{21}$$

where where n is an integer number, Δt is the discrete time interval used in the numerical integration scheme, while $\mathbf{Z}^n$ and $\mathbf{Z}^{n+1}$ respectively represent the numerical approximations of the exact solutions $\mathbf{z}^n = \mathbf{z}(t^n)$ and $\mathbf{z}^{n+1} = \mathbf{z}(t^{n+1})$ respectively defined at the discrete time instants $t^n = n\Delta t$ and $t^{n+1} = (n+1)\Delta t$. Another viable option is based on the use of the fourth-order explicit Runge-Kutta method which can be summarized in the following vector equation:

$$\mathbf{Z}^{n+1} = \mathbf{Z}^n + \Delta t \left(\frac{1}{6}\mathbf{Z}_1^n + \frac{1}{3}\mathbf{Z}_2^n + \frac{1}{3}\mathbf{Z}_3^n + \frac{1}{6}\mathbf{Z}_4^n \right) \tag{22}$$

where:

$$\begin{cases} \mathbf{Z}_1^n = \mathbf{f}(t^n, \mathbf{Z}^n) \\ \mathbf{Z}_2^n = \mathbf{f}(t^n + \frac{1}{2}\Delta t, \mathbf{Z}^n + \frac{1}{2}\mathbf{Z}_1^n) \\ \mathbf{Z}_3^n = \mathbf{f}(t^n + \frac{1}{2}\Delta t, \mathbf{Z}^n + \frac{1}{2}\mathbf{Z}_2^n) \\ \mathbf{Z}_4^n = \mathbf{f}(t^n + \Delta t, \mathbf{Z}^n + \mathbf{Z}_3^n) \end{cases} \tag{23}$$

Although they are both explicit integration algorithms, the relatively more complex Runge-Kutta numerical scheme is typically preferred to the simpler Euler forward formula because of its superior accuracy and its wider stability region. However, since the augmented formulation is an analytical technique for the determination of the system generalized acceleration vector based on an index-one set of DAEs, a constraint stabilization procedure is also required in order to eliminate the drift of the kinematic constraints at the position and velocity levels. The constraint stabilization procedure must be combined with the numerical integration scheme used for the progressive computation of the numerical solution on the discretized time axis.

C. Adjoint-Based Iterative Numerical Procedure for the Optimal Control Design

In this subsection, the principal equations that define the necessary conditions for the optimal control design of nonlinear control laws are presented. For this purpose, an iterative numerical procedure based on the adjoint equations can be mathematically formulated. The control method used in this research work originates from the theory of optimal control. This method can be applied to both linear and nonlinear dynamical systems. To this end, the derivation of a two-point boundary value problem formed by a set of nonlinear differential-algebraic equations is analytically formulated in this subsection and a numerical solution procedure is briefly described using the adjoint approach [58], [59].

As discussed in this subsection, the adjoint approach is an effective method for the numerical solution of general optimal control problems. This method is particularly useful in the case of nonlinear mechanical systems for which optimal control laws are difficult to determinate, such as the pantograph mechanism of interest for this study. The adjoint computational approach does not represent a single numerical algorithm. This method is grounded on a wider mathematical framework in which the nonlinear control problem can be reformulated and solved using a set of well-known numerical procedures. However, it is important to note that the adjoint methodology analyzed in this section can be applied to multibody mechanical systems characterized by a closed-loop structure, like the pantograph mechanism analyzed in this paper, because this method exploits the explicit form of the dynamic equations derived by using an augmented formulation approach applied to the dynamic analysis of constrained systems discussed in the previous subsection of the manuscript.

The adjoint method can be applied to the dynamic equations of multibody mechanical systems represented in the nonlinear state-space form. The goal of the adjoint method is to minimize a performance index denoted with J_c that mathematically represents the cost of the designed control laws. A general form of the performance index J_c, which is defined on the time interval from $t = 0$ to $t = T$, can be written as follows:

$$J_c = h_c|_T + \int_0^T g_c dt \tag{24}$$

where h_c represents a general function called terminal cost function whereas the arbitrary function g_c is called current cost function. For simplicity, the following quadratic structure for the terminal cost function h_c and for the current cost function g_c can be assumed:

$$h_c = \frac{1}{2}\mathbf{z}^T \mathbf{Q}_T \mathbf{z} \tag{25}$$

and

$$g_c = \frac{1}{2}\mathbf{z}^T \mathbf{Q}_z \mathbf{z} + \frac{1}{2}\mathbf{u}^T \mathbf{Q}_u \mathbf{u} + \frac{1}{2}\mathbf{F}^T \mathbf{Q}_F \mathbf{F} \tag{26}$$

where $\mathbf{u}$ is the input vector associated with the optimal control actions, $\mathbf{F}$ identifies a general vector of interactions (forces and moments) to be minimized, while $\mathbf{Q}_T$, $\mathbf{Q}_z$, $\mathbf{Q}_u$, and $\mathbf{Q}_F$ are constant positive-semidefinite weight matrices which are used by the control analyst to define in a straightforward manner the structure of the cost functional J_c. By introducing an additional vector denoted with $\mathbf{y}$, that is called adjoint state and has the same dimensions of the state vector $\mathbf{z}$, one can prove by employing the mathematical tools of the calculus of variation that the necessary conditions which minimize the cost functional J_c are given by:

$$\begin{cases} \dot{\mathbf{z}} = \mathbf{f}, \quad \mathbf{z}|_0 = \mathbf{z}_0 \\ \dot{\mathbf{y}} = -\mathbf{A}_c^T \mathbf{y} - \boldsymbol{\varphi}_c^T, \quad \mathbf{y}|_T = \boldsymbol{\eta}_c^T|_T \\ \mathbf{B}_c^T \mathbf{y} + \boldsymbol{\psi}_c^T = \mathbf{0} \end{cases} \tag{27}$$

where the sensitivity matrices $\mathbf{A}_c$ and $\mathbf{B}_c$ are respectively defined as:

$$\mathbf{A}_c = \frac{\partial \mathbf{f}}{\partial \mathbf{z}}, \quad \mathbf{B}_c = \frac{\partial \mathbf{f}}{\partial \mathbf{u}} \tag{28}$$

The sensitivity vectors $\boldsymbol{\eta}_c$ and $\boldsymbol{\varphi}_c$ are respectively given by:

$$\boldsymbol{\eta}_c = \frac{\partial h_c}{\partial \mathbf{z}} = \mathbf{z}^T \mathbf{Q}_T \tag{29}$$

and

$$\boldsymbol{\varphi}_c = \frac{\partial g_c}{\partial \mathbf{z}} = \mathbf{z}^T \mathbf{Q}_z + \mathbf{F}^T \mathbf{Q}_F \frac{\partial \mathbf{F}}{\partial \mathbf{z}} \tag{30}$$

The sensitivity vector $\boldsymbol{\psi}_c$ can be computed as follows:

$$\boldsymbol{\psi}_c = \frac{\partial g_c}{\partial \mathbf{u}} = \mathbf{u}^T \mathbf{Q}_u + \mathbf{F}^T \mathbf{Q}_F \frac{\partial \mathbf{F}}{\partial \mathbf{u}} \tag{31}$$

This set of differential-algebraic equations form a nonlinear two-point boundary value problem. This nonlinear problem represents a mathematical problem that can be numerically solved by using an iterative algorithm based on the adjoint approach.

D. Numerical Solution of the Adjoint Equations

In this subsection, the solution procedures devised for solving the adjoint equations associated with the nonlinear optimal control problem are concisely discussed. The first step of the iterative algorithm considered in this section is based on the numerical solution of the dynamic equations and of the adjoint equations assuming an initial guess of the optimal control law. For this purpose, one can search for an approximate solution of the optimal time laws that describes the vector of control actions $\mathbf{u}$ as follows:

$$\mathbf{U}^{r,k+1} = \mathbf{U}^{r,k} + \alpha^k \mathbf{D}^{r,k} \tag{32}$$

and

$$\alpha^k = \arg(\min_{\alpha}(J_c)) \tag{33}$$

where the superscript k indicates the iteration number of the adjoint procedure, $\mathbf{U}^r$ denotes the reshaped version of the family of discretized vectors $\mathbf{U}^n$ representing the numerical solution for the vector of control inputs $\mathbf{u}^n = \mathbf{u}(t^n)$ defined at each time step t^n, $\mathbf{D}^r$ corresponds to the reshaped version of the family of direction vectors $\mathbf{D}^n$ identifying a direction along which the line search in the minimization procedure is performed, and α is a line parameter. For example, the vector $\mathbf{U}^r$ is assembled as follows:

$$\mathbf{U}^r = \begin{bmatrix} \mathbf{U}^0 \\ \mathbf{U}^1 \\ \vdots \\ \mathbf{U}^n \\ \vdots \\ \mathbf{U}^{N-1} \\ \mathbf{U}^N \end{bmatrix} \tag{34}$$

where N is the number of time intervals that form the equispaced discretization of the time axis. There are several numerical methods that can be used for determining the search direction $\mathbf{D}^n$. One of the most effective approaches is based on the nonlinear conjugate gradient scheme in which the search direction follows an optimized pattern associated with the gradient of the cost function $\mathbf{G}^n$ given by:

$$\mathbf{D}^{n,k} = -\mathbf{G}^{n,k-1} + \mathbf{E}^{n,k-1} \tag{35}$$

where:

$$\begin{cases} \mathbf{G}^{n,k} = \left(\boldsymbol{\psi}_c^{n,k}\right)^T + \left(\mathbf{B}_c^{n,k}\right)^T \mathbf{Y}^{n,k} \\ \mathbf{E}^{n,k-1} = \beta^{n,k} \mathbf{D}^{n,k-1} \end{cases} \tag{36}$$

where the vector $\mathbf{E}^n$ is a correction term associated with the search direction vector $\mathbf{D}^n$, $\mathbf{Y}^{n,k}$ is the numerical approximation of the exact solutions for the adjoint state $\mathbf{y}^n = \mathbf{y}(t^n)$ obtained at the iteration k, and β is a scalar parameter associated with a given choice of the search direction used during the iteration process. In the simple steepest descent algorithm, the search parameter β is set equal to zero. However, in general, this choice is not convenient because it is sensible to the variation of curvature of the cost function J_c leading to a zigzagging behavior of the minimization algorithm. On the other hand, an appropriate selection of the parameter β can effectively solve this issue. For this purpose, several efficient algorithms called with the names of their developers can be found in the literature. The principal methods used in the nonlinear conjugate gradient optimization algorithm for computing the search parameter β are given by:

$$\begin{cases} \beta_{FR}^{n,k} = \frac{\left(\mathbf{G}^{n,k}\right)^T \mathbf{G}^{n,k}}{\left(\mathbf{G}^{n,k-1}\right)^T \mathbf{G}^{n,k-1}} \\ \beta_{PR}^{n,k} = \frac{\left(\mathbf{G}^{n,k}\right)^T \left(\mathbf{G}^{n,k} - \mathbf{G}^{n,k-1}\right)}{\left(\mathbf{G}^{n,k-1}\right)^T \mathbf{G}^{n,k-1}} \\ \beta_{HS}^{n,k} = -\frac{\left(\mathbf{G}^{n,k}\right)^T \left(\mathbf{G}^{n,k} - \mathbf{G}^{n,k-1}\right)}{\left(\mathbf{D}^{n,k-1}\right)^T \left(\mathbf{G}^{n,k} - \mathbf{G}^{n,k-1}\right)} \\ \beta_{DY}^{n,k} = -\frac{\left(\mathbf{G}^{n,k}\right)^T \mathbf{G}^{n,k}}{\left(\mathbf{D}^{n,k-1}\right)^T \left(\mathbf{G}^{n,k} - \mathbf{G}^{n,k-1}\right)} \end{cases} \tag{37}$$

where β_{FR}, β_{PR}, β_{HS}, and β_{DY} respectively represent the direction parameters used in the Fletcher-Reeves, Polak-Ribiere, Hestenes-Stiefel, and Dai-Yuan search algorithms [60]. In the development of an iterative algorithm based on the adjoint approach, one can determine an optimal distribution in time of the feedforward control action that converges to an appropriate time law when a prescribed tolerance on the performance index J_c is reached. To this end, a numerical approximation of the performance index J_c can be found at each iteration k of the optimization procedure by using an integration scheme. For example, the following trapezoidal integration algorithm can be employed for performing this task:

$$\begin{aligned} J_c &= h_c(\mathbf{z}, t)|_T + \int_0^T g_c(\mathbf{z}, \mathbf{u}, t) dt \\ &= h_c(\mathbf{z}, t)|_T + \sum_{n=0}^{N-1} \int_{t^n}^{t^{n+1}} g_c(\mathbf{z}, \mathbf{u}, t) dt \\ &\simeq h_c(\mathbf{Z}^N, T) + \tfrac{\Delta t}{2} \sum_{n=0}^{N-1} g_c(\mathbf{Z}^n, \mathbf{U}^n, t^n) \\ &\quad + \tfrac{\Delta t}{2} \sum_{n=0}^{N-1} g_c(\mathbf{Z}^{n+1}, \mathbf{U}^{n+1}, t^{n+1}) \end{aligned} \tag{38}$$

Moreover, the adjoint equations can be solved by using the same numerical schemes available for the solution of the dynamic equations since the former equations are ODEs. The adjoint equations can be rewritten in the following compact form:

$$\dot{\mathbf{y}} = \mathbf{g} \tag{39}$$

where the nonlinear vector function $\mathbf{g}$ represents the adjoint state function defined as:

$$\mathbf{g} = -\mathbf{A}_c^T \mathbf{y} - \boldsymbol{\varphi}_c^T \tag{40}$$

In the numerical solution of the adjoint equations, the time marching is reversed from the final instant of time $t = T$ to

the initial instant of time $t = 0$. A simple numerical method that can be used for solving the adjoint equations is the explicit Euler method described by the following integration scheme:

$$\mathbf{Y}^{n-1} = \mathbf{Y}^{n} - \Delta t \mathbf{g}(t^{n}, \mathbf{Y}^{n}) \tag{41}$$

where Δt is the time step used in the numerical integration of the adjoint equations, whereas $\mathbf{Y}^{n}$ and $\mathbf{Y}^{n-1}$ respectively represent the numerical approximation of the exact solutions $\mathbf{y}^{n} = \mathbf{y}(t^{n})$ and $\mathbf{y}^{n-1} = \mathbf{y}(t^{n-1})$ respectively defined at the discrete time instants $t^{n} = n\Delta t$ and $t^{n-1} = (n-1)\,\Delta t$. In the numerical solution of the adjoint equations, one can also implement the following explicit Runge-Kutta integration algorithm in order to increase the accuracy of the numerical solution from the first order to the fourth order:

$$\mathbf{Y}^{n-1} = \mathbf{Y}^{n} - \Delta t \left(\frac{1}{6}\mathbf{Y}_{1}^{n} + \frac{1}{3}\mathbf{Y}_{2}^{n} + \frac{1}{3}\mathbf{Y}_{3}^{n} + \frac{1}{6}\mathbf{Y}_{4}^{n} \right) \tag{42}$$

where:

$$\begin{cases} \mathbf{Y}_{1}^{n} = \mathbf{g}(t^{n}, \mathbf{Y}^{n}) \\ \mathbf{Y}_{2}^{n} = \mathbf{g}(t^{n} - \frac{1}{2}\Delta t, \mathbf{Y}^{n} + \frac{1}{2}\mathbf{Y}_{1}^{n}) \\ \mathbf{Y}_{3}^{n} = \mathbf{g}(t^{n} - \frac{1}{2}\Delta t, \mathbf{Y}^{n} + \frac{1}{2}\mathbf{Y}_{2}^{n}) \\ \mathbf{Y}_{4}^{n} = \mathbf{g}(t^{n} - \Delta t, \mathbf{Y}^{n} + \mathbf{Y}_{3}^{n}) \end{cases} \tag{43}$$

In the computational procedure used for solving the adjoint equations, the approximate solution obtained for the state vector $\mathbf{z}$ that appears in the sensitivity vector $\boldsymbol{\varphi}_{c}$ plays the role of a forcing function. This forcing function is generated by the numerical approximation of the vector of control law $\mathbf{u}$ obtained at a given iteration k of the trial-and-error numerical procedure employed for optimizing the feedforward controller. From practical considerations, one can observe that it is convenient to use the same integration algorithm for solving both the dynamic equations and the adjoint equations referred to the same discretization of the time axis performed employing a constant step size.

III. Demonstrative Example: Dynamics of the Kinematically-Driven Double Inverted Pendulum

In this section, a dynamical model of a kinematically-driven double inverted pendulum system is formulated by using the multibody formulation approach adopted in the paper. Furthermore, a set of numerical results found by means of dynamical simulations is also discussed in this section. The simple multibody model developed in this section is used for demonstrating the fundamental aspects of the analytical approach devised in this paper considering a simple mechanical system characterized by a moving component having an imposed motion. To this end, the set of numerical results presented in this section concern the output motion of the double pendulum resulting from an input motion assigned to the cart.

A. Dynamic Equations of the Kinematically-Driven Double Inverted Pendulum

In this subsection, the two-dimensional dynamic model of the kinematically-driven double inverted pendulum considered in this work is presented. For this purpose, the fundamental equations of classical mechanics are used for the derivation of a mechanical model of the double inverted pendulum system employing a Lagrangian approach. This approach is based on an augmented set of Lagrangian co-ordinates that simplifies the mathematical modeling of the double inverted pendulum system. For the correct derivation of the equations of motion, which in this simplified case are nonlinear ordinary differential equations, one needs to take into account all the dynamic effects that are significant for the nonlinear analysis. In particular, the system mass matrix, the system inertial quadratic velocity vector, the system kinematically-driven generalized force vector, and the system generalized external force vector must be computed for all the bodies that form the mechanical system. For this purpose, the nonlinear dynamic equations analytically found in this work are obtained in the case of the dynamic analysis of the kinematically-driven double inverted pendulum system.

The schematic model of the kinematically-driven double inverted pendulum employed as an illustrative example is represented in Figure 1. The numerical data employed for

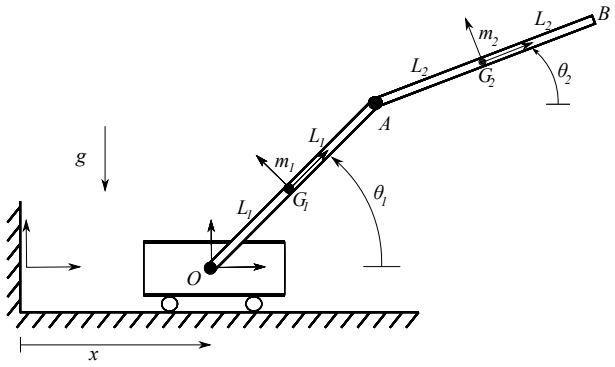

Fig. 1. Double inverted pendulum model.

modeling the kinematically-driven double inverted pendulum are reported in Table I. A rigid two-dimensional multibody model of the kinematically-drive double inverted pendulum is elaborated in this subsection. For this purpose, the kinematic equations that describe the topological structure of the double inverted pendulum are obtained first. The double inverted pendulum is formed by two mono-dimensional rigid bodies of length $2L_i$ and mass m_i, where the subscript i denotes the body number. The two rigid bodies that represent the mechanical components of the double inverted pendulum system are constrained by two kinematic joints, namely, two revolute joints respectively collocated in the point O and A of Figure 1. By considering a semi-recursive approach, the multibody dynamic equations can be derived by using the following generalized coordinate vector:

$$\mathbf{q} = \begin{bmatrix} \theta_1 \\ \theta_2 \end{bmatrix} \tag{44}$$

where θ_1 and θ_2 respectively represent the angular displacements of the first end second pendulum. On the other hand, for simplicity, it is assumed that the linear displacement of the cart denoted with x is imposed considering the following analytical function:

$$x = X_0 \sin(\Omega t) \tag{45}$$

TABLE I
DOUBLE INVERTED PENDULUM PARAMETERS.

Descriptions	Symbols	Data (units)
First Pendulum Half Length	L_1	$0.1\,(\mathrm{m})$
Second Pendulum Half Length	L_2	$0.2\,(\mathrm{m})$
First Pendulum Mass	m_1	$3\,(\mathrm{kg})$
Second Pendulum Mass	m_2	$4\,(\mathrm{kg})$
First Pendulum Mass Moment of Inertia	$I_{zz,1}$	$0.01\,(\mathrm{kg}{*}\mathrm{m}^2)$
Second Pendulum Mass Moment of Inertia	$I_{zz,2}$	$0.05333\,(\mathrm{kg}{*}\mathrm{m}^2)$
Gravitational Acceleration	g	$9.807\,(\mathrm{m/s}^2)$
Imposed Displacement Amplitude	X_0	$0.5\,(\mathrm{m})$
Imposed Displacement Angular Frequency	Ω	$0.9425\,(\mathrm{rad/s})$

where X_0 identifies the amplitude of the imposed displacement, while Ω indicates the imposed angular frequency of the motion assigned to the cart. It follows that:

$$\dot{x} = \Omega X_0 \cos(\Omega t), \quad \ddot{x} = -\Omega^2 X_0 \sin(\Omega t) \tag{46}$$

The global position vectors of the first and second pendulum centers of mass G_1 and G_2 are respectively denoted with $\mathbf{R}_1$ and $\mathbf{R}_2$ and are respectively defined as follows:

$$\mathbf{R}_1 = \begin{bmatrix} x + L_1\cos(\theta_1) \\ L_1\sin(\theta_1) \end{bmatrix} \tag{47}$$

$$\mathbf{R}_2 = \begin{bmatrix} x + 2L_1\cos(\theta_1) + L_2\cos(\theta_2) \\ 2L_1\sin(\theta_1) + L_2\sin(\theta_2) \end{bmatrix} \tag{48}$$

The global velocity vectors of the first and second pendulum centers of mass G_1 and G_2 are respectively denoted with $\dot{\mathbf{R}}_1$ and $\dot{\mathbf{R}}_2$ and are respectively defined as follows:

$$\dot{\mathbf{R}}_1 = \begin{bmatrix} \dot{x} - L_1\sin(\theta_1)\dot{\theta}_1 \\ L_1\cos(\theta_1)\dot{\theta}_1 \end{bmatrix} \tag{49}$$

$$\dot{\mathbf{R}}_2 = \begin{bmatrix} \dot{x} - 2L_1\sin(\theta_1)\dot{\theta}_1 - L_2\sin(\theta_2)\dot{\theta}_2 \\ 2L_1\cos(\theta_1)\dot{\theta}_1 + L_2\cos(\theta_2)\dot{\theta}_2 \end{bmatrix} \tag{50}$$

The Jacobian matrices of the first and second pendulum center of mass velocity vectors are respectively denoted with $\mathbf{J}_1$ and $\mathbf{J}_2$ and are respectively given by:

$$\mathbf{J}_1 = \frac{\partial \dot{\mathbf{R}}_1}{\partial \dot{\mathbf{q}}} = \begin{bmatrix} -L_1\sin(\theta_1) & 0 \\ L_1\cos(\theta_1) & 0 \end{bmatrix} \tag{51}$$

$$\mathbf{J}_2 = \frac{\partial \dot{\mathbf{R}}_2}{\partial \dot{\mathbf{q}}} = \begin{bmatrix} -2L_1\sin(\theta_1) & -L_2\sin(\theta_2) \\ 2L_1\cos(\theta_1) & L_2\cos(\theta_2) \end{bmatrix} \tag{52}$$

The additional vector terms of the first and second pendulum center of mass velocity vectors are respectively denoted with $\mathbf{v}_1$ and $\mathbf{v}_2$ and are respectively given by:

$$\mathbf{v}_1 = \mathbf{v}_2 = \begin{bmatrix} \dot{x} \\ 0 \end{bmatrix} \tag{53}$$

The angular velocities of the first and second pendulum are respectively denoted with ω_1 and ω_2 and are respectively equal to:

$$\omega_1 = \dot{\theta}_1, \quad \omega_2 = \dot{\theta}_2 \tag{54}$$

The Jacobian matrices of the first and second pendulum angular velocities are respectively denoted with $\mathbf{\Omega}_1$ and $\mathbf{\Omega}_2$ and are respectively equal to:

$$\mathbf{\Omega}_1 = \frac{\partial \omega_1}{\partial \dot{\mathbf{q}}} = \begin{bmatrix} 1 & 0 \end{bmatrix} \tag{55}$$

$$\mathbf{\Omega}_2 = \frac{\partial \omega_2}{\partial \dot{\mathbf{q}}} = \begin{bmatrix} 0 & 1 \end{bmatrix} \tag{56}$$

The additional vector terms of the first and second pendulum angular velocities are respectively denoted with $\mathbf{w}_1$ and $\mathbf{w}_2$ and are respectively defined as:

$$\mathbf{w}_1 = \mathbf{w}_2 = 0 \tag{57}$$

On the other hand, the dynamic equations of the kinematically-drive double inverted pendulum can be obtained employing the fundamental analytical methods of Lagrangian dynamics to yield:

$$\mathbf{M}\ddot{\mathbf{q}} = \mathbf{Q}_b \tag{58}$$

where $\mathbf{M}$ indicates the total mass matrix of the double inverted pendulum, whereas $\mathbf{Q}_b$ is the total generalized force vector acting on the dynamical system. The total system mass matrix $\mathbf{M}$ can be computed as follows:

$$\mathbf{M} = \mathbf{M}_1 + \mathbf{M}_2 \tag{59}$$

where $\mathbf{M}_1$ and $\mathbf{M}_2$ are respectively the mass matrices of the first and second pendulum that are respectively given by:

$$\begin{aligned} \mathbf{M}_1 &= m_1\mathbf{J}_1^T\mathbf{J}_1 + I_{zz,1}\mathbf{\Omega}_1^T\mathbf{\Omega}_1 \\ &= \begin{bmatrix} m_1L_1^2 + I_{zz,1} & 0 \\ 0 & 0 \end{bmatrix} \end{aligned} \tag{60}$$

$$\begin{aligned} \mathbf{M}_2 &= m_2\mathbf{J}_2^T\mathbf{J}_2 + I_{zz,2}\mathbf{\Omega}_2^T\mathbf{\Omega}_2 \\ &= \begin{bmatrix} 4m_2L_1^2 & 2L_1L_2m_2\cos(\theta_{1,2}) \\ 2L_1L_2m_2\cos(\theta_{1,2}) & m_2L_2^2 + I_{zz,2} \end{bmatrix} \end{aligned} \tag{61}$$

where $\theta_{1,2} = \theta_1 - \theta_2$. In the case of the double inverted pendulum system, the quadratic part of the system kinetic energy T_q can be explicitly determined as follows:

$$\begin{aligned} T_q &= \tfrac{1}{2}\dot{\mathbf{q}}^T\mathbf{M}\dot{\mathbf{q}} \\ &= \tfrac{1}{2}\left((m_1 + 4m_2)L_1^2 + I_{zz,1}\right)\dot{\theta}_1^2 \\ &\quad + 2L_1L_2m_2\cos(\theta_1 - \theta_2)\dot{\theta}_1\dot{\theta}_2 \\ &\quad + \tfrac{1}{2}\left(m_2L_2^2 + I_{zz,2}\right)\dot{\theta}_2^2 \end{aligned} \tag{62}$$

The inertia quadratic velocity vector of the double pendulum system $\mathbf{Q}_v$ can be obtained from the quadratic part of the system kinetic energy T_q and considering the time derivative of the system mass matrix $\dot{\mathbf{M}}$ as follows:

$$\mathbf{Q}_v = \left(\frac{\partial T_q}{\partial \mathbf{q}}\right)^T - \dot{\mathbf{M}}\dot{\mathbf{q}} = \begin{bmatrix} -m_2L_1L_2\sin(\theta_{1,2})\dot{\theta}_2^2 \\ m_2L_1L_2\sin(\theta_{1,2})\dot{\theta}_1^2 \end{bmatrix} \tag{63}$$

The multiplicative vector associated with the linear part of the kinetic energy of the double inverted pendulum $\mathbf{b}$ is given by:

$$\mathbf{b} = \mathbf{b}_1 + \mathbf{b}_2 \tag{64}$$

where $\mathbf{b}_1$ and $\mathbf{b}_2$ are respectively the multiplicative vectors associated with the linear part of the kinetic energy of the first and second pendulum that are respectively defined as:

$$\begin{aligned}\mathbf{b}_1 &= 2m_1\mathbf{J}_1^T\mathbf{v}_1 + 2I_{zz,1}\mathbf{\Omega}_1^T\mathbf{w}_1 \\ &= \begin{bmatrix} -2m_1L_1\sin(\theta_1)\dot{x} \\ 0 \end{bmatrix}\end{aligned} \tag{65}$$

$$\begin{aligned}\mathbf{b}_2 &= 2m_2\mathbf{J}_2^T\mathbf{v}_2 + 2I_{zz,2}\mathbf{\Omega}_2^T\mathbf{w}_2 \\ &= \begin{bmatrix} -4m_2L_1\sin(\theta_1)\dot{x} \\ -2m_2L_2\sin(\theta_2)\dot{x} \end{bmatrix}\end{aligned} \tag{66}$$

The linear part of the kinetic energy of the double inverted pendulum T_l is equal to:

$$\begin{aligned}T_l &= \tfrac{1}{2}\mathbf{b}^T\dot{\mathbf{q}} \\ &= -\left(m_1 + 2m_2\right)L_1\sin(\theta_1)\dot{\theta}_1\dot{x} \\ &\quad -m_2L_2\sin(\theta_2)\dot{\theta}_2\dot{x}\end{aligned} \tag{67}$$

The additional scalar term associated with the scalar part of the kinetic energy of the double inverted pendulum c can be computed as follows:

$$c = c_1 + c_2 \tag{68}$$

where c_1 and c_2 are respectively the additional scalar terms associated with the scalar part of the kinetic energy of the first and second pendulum that are respectively given by:

$$c_1 = m_1\mathbf{v}_1^T\mathbf{v}_1 + I_{zz,1}\mathbf{w}_1^T\mathbf{w}_1 = m_1\dot{x}^2 \tag{69}$$

$$c_2 = m_2\mathbf{v}_2^T\mathbf{v}_2 + I_{zz,2}\mathbf{w}_2^T\mathbf{w}_2 = m_2\dot{x}^2 \tag{70}$$

The scalar part of the kinetic energy of the double inverted pendulum T_c is equal to:

$$T_c = \frac{1}{2}c = \frac{1}{2}\left(m_1 + m_2\right)\dot{x}^2 \tag{71}$$

Once that the linear part T_l and the scalar part T_c of the system kinetic energy are known, the kinetic energy induced by the kinematically-driven motion T_m of the double inverted pendulum can be simply computed as:

$$\begin{aligned}T_m &= T_l + T_c \\ &= -\left(m_1 + 2m_2\right)L_1\sin(\theta_1)\dot{\theta}_1\dot{x} \\ &\quad -m_2L_2\sin(\theta_2)\dot{\theta}_2\dot{x} + \tfrac{1}{2}\left(m_1 + m_2\right)\dot{x}^2\end{aligned} \tag{72}$$

The kinematically-driven generalized force vector of the double pendulum system $\mathbf{Q}_m$ can be obtained from the kinetic energy induced by the kinematically-driven motion T_m as follows:

$$\begin{aligned}\mathbf{Q}_m &= \left(\tfrac{\partial T_m}{\partial \mathbf{q}}\right)^T - \tfrac{d}{dt}\left(\tfrac{\partial T_m}{\partial \dot{\mathbf{q}}}\right)^T \\ &= \begin{bmatrix} L_1\left(m_1 + 2m_2\right)\sin(\theta_1)\ddot{x} \\ L_2m_2\sin(\theta_2)\ddot{x} \end{bmatrix}\end{aligned} \tag{73}$$

On the other hand, the total potential energy of the double inverted pendulum system is given by:

$$U = U_1 + U_2 \tag{74}$$

where U_1 and U_2 respectively represent the gravitational potential energy of the first and second pendulum that can be readily determined as:

$$U_1 = m_1g\mathbf{j}^T\mathbf{R}_1 = m_1gL_1\sin(\theta_1) \tag{75}$$

$$U_2 = m_2g\mathbf{j}^T\mathbf{R}_2 = 2m_2gL_1\sin(\theta_1) + m_2gL_2\sin(\theta_2) \tag{76}$$

The generalized external force vector of the double pendulum system associated with the gravity force field $\mathbf{Q}_e$ is equal to:

$$\mathbf{Q}_e = -\left(\frac{\partial U}{\partial \mathbf{q}}\right)^T = \begin{bmatrix} -\left(m_1 + 2m_2\right)gL_1\cos(\theta_1) \\ -m_2gL_2\cos(\theta_2) \end{bmatrix} \tag{77}$$

Finally, one can write the analytical form of the total body generalized force vector of the double pendulum system $\mathbf{Q}_b$ as follows:

$$\begin{aligned}\mathbf{Q}_b &= \mathbf{Q}_v + \mathbf{Q}_m + \mathbf{Q}_e \\ &= \begin{bmatrix} -m_2L_1L_2\sin(\theta_{1,2})\dot{\theta}_2^2 \\ +L_1m_{1,2}\sin(\theta_1)\ddot{x} \\ -m_{1,2}gL_1\cos(\theta_1) \\ \\ m_2L_1L_2\sin(\theta_{1,2})\dot{\theta}_1^2 \\ +L_2m_2\sin(\theta_2)\ddot{x} \\ -m_2gL_2\cos(\theta_2) \end{bmatrix}\end{aligned} \tag{78}$$

where $m_{1,2} = m_1 + 2m_2$. The dynamic equations reported in this subsection completely describe the total system mass matrix $\mathbf{M}$ and the total system generalized force vector $\mathbf{Q}_b$ of the double inverted pendulum system considered in the paper as a demonstrative example.

B. Dynamic Analysis of the Kinematically-Driven Double Inverted Pendulum

In this subsection, the dynamic analysis of the double inverted pendulum system is reported. For this purpose, the numerical scheme used to solve the nonlinear equations of motion is the fourth-order explicit Runge-Kutta method. Figure 2(a) shows the angular displacement of the first pendulum of the double inverted pendulum system whose time evolution is induced by the kinematically-driven motion, while Figure 2(b) represents the corresponding angular velocity. Figure 3(a) shows the angular displacement of thesecond pendulum of the double inverted pendulum system whose time evolution is induced by the kinematically-driven motion, while Figure 3(b) represents the corresponding angular velocity. The planar trajectory of the extremal point B of Figure 1 collocated at the tip of the double inverted pendulum system is represented in Figure 4. The horizontal displacement of the tip point B of the double inverted pendulum system is represented in Figure 5(a), while the vertical displacement of the same point is shown in Figure 5(b). The horizontal velocity of the tip point B of the double inverted pendulum system is represented in Figure 6(a), while the vertical velocity of the same point is shown in Figure 6(b). The numerical results presented in this subsection demonstrate the effectiveness of the method devised in this investigation for describing the dynamical behavior of mechanical systems animated by a kinematically-driven motion.

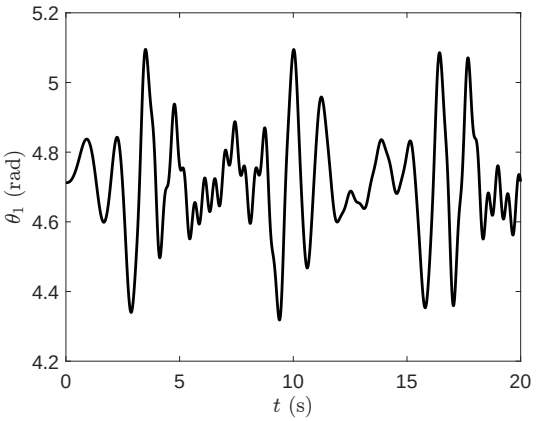

(a) First pendulum angular displacement.

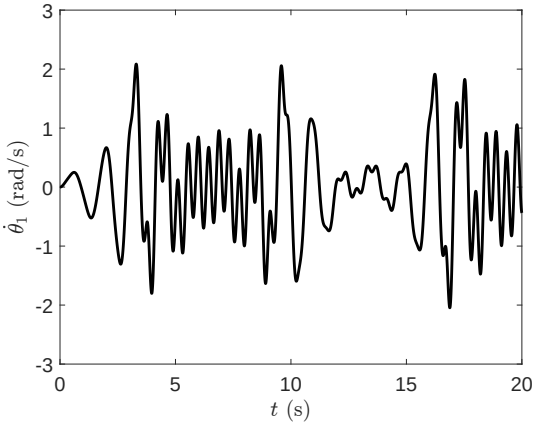

(b) First pendulum angular velocity.

Fig. 2. First pendulum dynamical evolution.

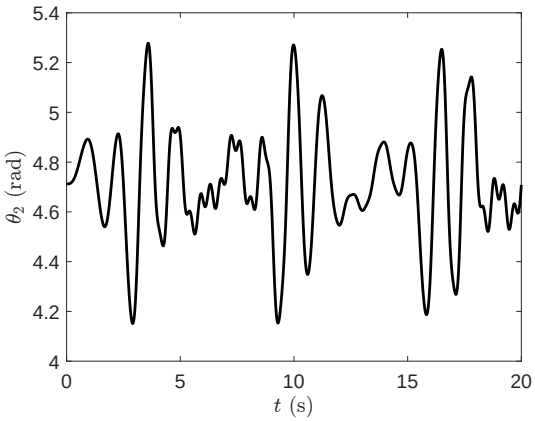

(a) Second pendulum angular displacement.

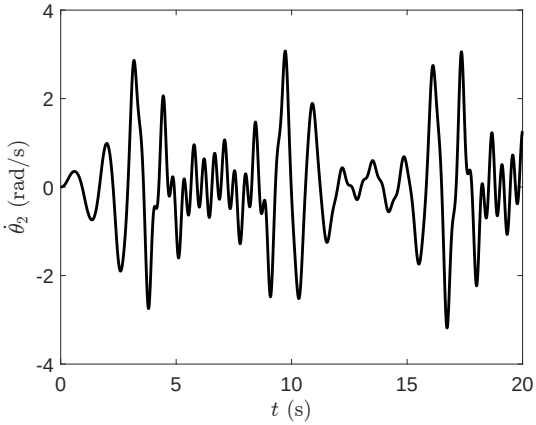

(b) Second pendulum angular velocity.

Fig. 3. Second pendulum dynamical evolution.

IV. Case Study: Dynamics and Control of the Pantograph Mechanism

In this section, a dynamical model of the pantograph mechanism is presented considering a multibody formulation approach. The numerical results found using the approach developed in this investigation are also discussed in this section. The multibody model developed in this section is used for performing numerical experiments on the dynamic behavior of the pantograph mechanism interacting with the catenary cable. In particular, a set of numerical results deriving from the multibody-based modeling technique used in this investigation and the nonlinear adjoint-based control strategy developed in the paper are presented. For this purpose, the numerical results that originate from the design of an open-loop controller for the optimal time law of the control actuator are presented.

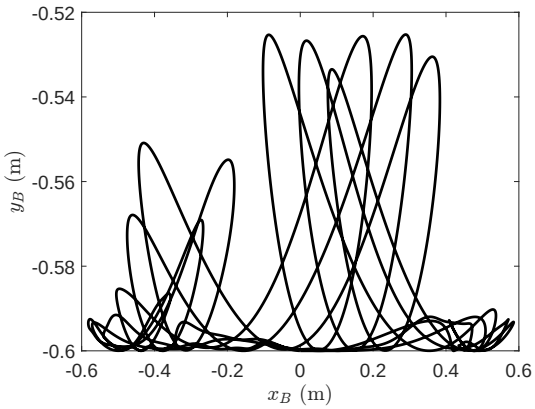

Fig. 4. Planar trajectory of the tip point of the double inverted pendulum system.

A. Unconstrained Dynamic Equations of the Pantograph Mechanism

In this subsection, the two-dimensional dynamic model of the pantograph mechanism considered in this work is presented. To this end, the fundamental equations of classical mechanics are used for the derivation of a mechanical model of the pantograph system employing a Lagrangian approach. This approach is based on an augmented set of Lagrangian coordinates that facilitates the geometric description of the pantograph model. In order to correctly derive the multibody differential-algebraic dynamic equations, it is necessary to consider all the dynamic effects that are relevant for the description of the nonlinear analysis of the pantograph mechanism. In particular, considering a recursive procedure, the system mass matrix, the system generalized inertia effects, and the external force vector can be computed by using the methods of analytical mechanics applied separately to each rigid body that composes the pantograph mechanism. To this end, the nonlinear dynamic equations used in this work for describing the time evolution of the mechanical system that models the pantograph mechanism are obtained

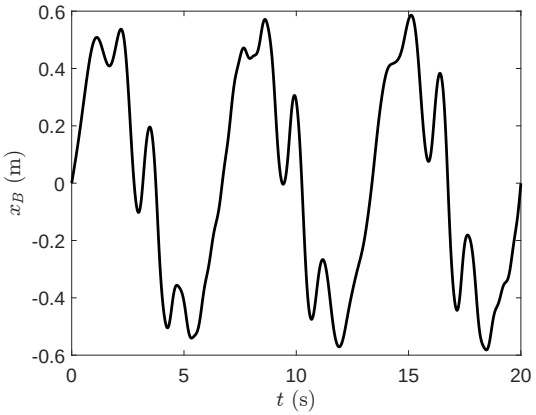

(a) Tip point horizontal displacement.

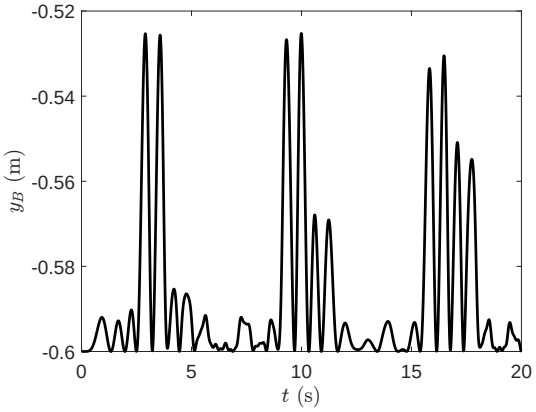

(b) Tip point vertical displacement.

Fig. 5. Horizontal and vertical displacement of the tip point of the double inverted pendulum system.

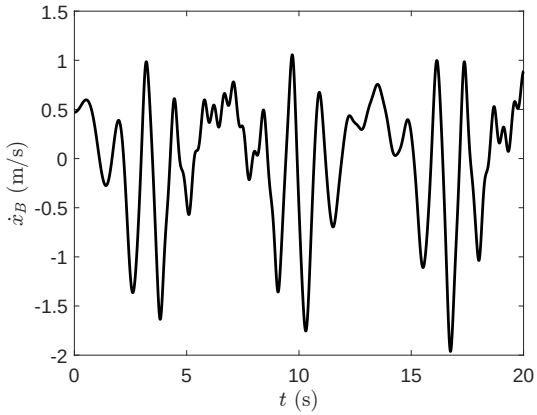

(a) Tip point horizontal velocity.

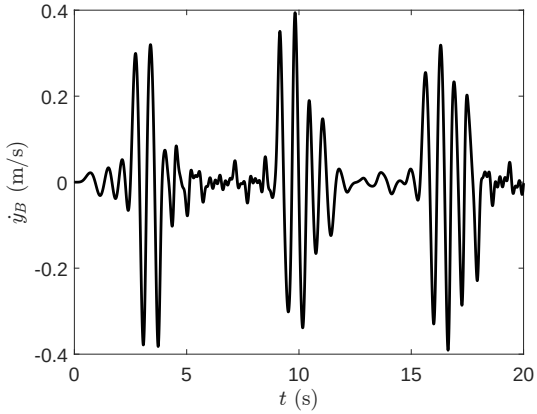

(b) Tip point vertical velocity.

Fig. 6. Horizontal and vertical velocity of the tip point of the double inverted pendulum system.

using the fundamental principles of classical mechanics. Subsequently, the resulting multibody model that mathematically defines the differential-algebraic dynamic equations of the pantograph and the catenary coupled systems is treated by using the augmented formulation. By doing so, the numerical techniques for the computation of optimal control actions can be readily employed for the design of a nonlinear controller that serves for the attenuation of the contact forces generated between the pantograph and the catenary.

The geometrical model of the pantograph mechanism considered in this investigation is represented in Figure 7. The numerical data used for modeling the pantograph mechanism are reported in Table II. A rigid two-dimensional multibody model of the pantograph mechanism is elaborated in this subsection. For this purpose, the kinematic equations that describe the topological structure of the pantograph mechanism are obtained by means of simple geometric constructions. The pantograph mechanism is formed by five mono-dimensional rigid bodies of length $2L_i$ and mass m_i, where the subscript i denotes the body number. The five rigid bodies that represent the mechanical components of the pantograph system are constrained by six kinematic joints, namely four revolute joints respectively collocated in the points O, A, B, and C, one rigid joint collocated in the point C, and one prismatic joint collocated in the point D of Figure 7. The pneumatic actuator that provides the lift force to the pantograph is modeled as a nonlinear spring-damper-force actuator having a stiffness coefficient k_1, a viscous

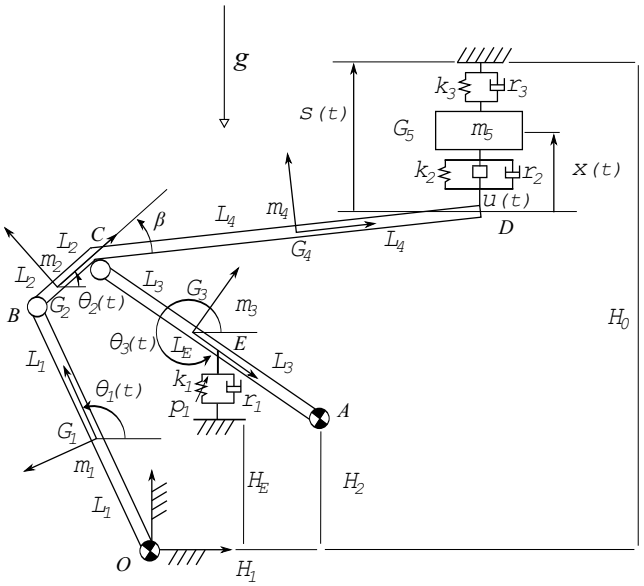

Fig. 7. Pantograph mechanism model.

damping coefficient r_1, and a positive constant force p_1. The suspension mechanism is modeled as a spring-damper element featuring a stiffness coefficient k_2 and a viscous damping coefficient r_2. The catenary wire is schematized considering an elastic force field having a stiffness coefficient k_3 and a viscous damping coefficient r_3. By considering a

TABLE II
PANTOGRAPH MECHANISM PARAMETERS.

Descriptions	Symbols	Data (units)
Thrust Rod Half Length	L_1	0.700 (m)
Crank Half Length	L_2	0.110 (m)
Lower Arm Half Length	L_3	0.850 (m)
Upper Arm Half Length	L_4	0.950 (m)
Moving Support Reference Height	H_0	2.635 (m)
Ground Revolute Joint Horizontal Position	H_1	0.200 (m)
Ground Revolute Joint Vertical Position	H_2	0.140 (m)
Pneumatic Actuator Reference Height	H_E	0.140 (m)
Pneumatic Actuator Local Distance	L_E	0.500 (m)
Crank - Upper Arm Fixed Angle	β	0.209 (rad)
Thrust Rod Mass	m_1	2.000 (kg)
Crank Mass	m_2	1.038 (kg)
Lower Arm Mass	m_3	1.038 (kg)
Upper Arm Mass	m_4	8.962 (kg)
Pan-Head Mass	m_5	0.500 (kg)
Gravitational Acceleration	g	9.810 (m/s^2)
Pneumatic Actuator Lift Force	p_1	1000.000 (N)
Pneumatic Actuator Stiffness	k_1	100.000 (N/m)
Pneumatic Actuator Damping	r_1	1.000 (N $*$ s/m)
Suspension System Stiffness	k_2	200.000 (N/m)
Suspension System Damping	r_2	2.000 (N $*$ s/m)
Pantograph/Catenary Stiffness	k_3	300.000 (N/m)
Pantograph/Catenary Damping	r_3	3.000 (N $*$ s/m)

semi-recursive approach originating from the kinematic chain rule, the multibody dynamic equations of the closed-loop mechanism can be obtained employing the following vector of generalized coordinates:

$$\mathbf{q} = \begin{bmatrix} \theta_1 \\ \theta_2 \\ \theta_3 \\ x \end{bmatrix} \tag{79}$$

where θ_1, θ_2, and θ_3 represent the angular displacements of the pantograph arms, whereas x indicates the displacement of the pantographs pan-head. The mathematical form of the dynamic equations of the pantograph mechanism is amenable to be treated with a standard mechanical method for the explicit determination of the generalized constraint forces based on the augmented formulation. Therefore, the dynamic equations of the unconstrained mechanism can be deduced using the fundamental analytical methods of Lagrangian dynamics as follows:

$$\mathbf{M}\ddot{\mathbf{q}} = \mathbf{Q}_b \tag{80}$$

where $\mathbf{M}$ indicates the total mass matrix of the pantograph mechanism, whereas $\mathbf{Q}_b$ is the total generalized force vector acting on the dynamical system. The total system mass matrix $\mathbf{M}$ can be computed as follows:

$$\mathbf{M} = \mathbf{M}_1 + \mathbf{M}_2 + \mathbf{M}_3 + \mathbf{M}_4 + \mathbf{M}_5 \tag{81}$$

where $\mathbf{M}_1$, $\mathbf{M}_2$, $\mathbf{M}_3$, $\mathbf{M}_4$, and $\mathbf{M}_5$ are the mass matrices of the rigid bodies that form the rigid mechanism which are respectively defined as:

$$\mathbf{M}_1 = \begin{bmatrix} \mathbf{M}_1^{1,1} & 0 & 0 & 0 \\ 0 & 0 & 0 & 0 \\ 0 & 0 & 0 & 0 \\ 0 & 0 & 0 & 0 \end{bmatrix} \tag{82}$$

$$\mathbf{M}_2 = \begin{bmatrix} \mathbf{M}_2^{1,1} & \mathbf{M}_2^{1,2} & 0 & 0 \\ \mathbf{M}_2^{2,1} & \mathbf{M}_2^{2,2} & 0 & 0 \\ 0 & 0 & 0 & 0 \\ 0 & 0 & 0 & 0 \end{bmatrix} \tag{83}$$

$$\mathbf{M}_3 = \begin{bmatrix} \mathbf{M}_3^{1,1} & \mathbf{M}_3^{1,2} & \mathbf{M}_3^{1,3} & 0 \\ \mathbf{M}_3^{2,1} & \mathbf{M}_3^{2,2} & \mathbf{M}_3^{2,3} & 0 \\ \mathbf{M}_3^{3,1} & \mathbf{M}_3^{3,2} & \mathbf{M}_3^{3,3} & 0 \\ 0 & 0 & 0 & 0 \end{bmatrix} \tag{84}$$

$$\mathbf{M}_4 = \begin{bmatrix} \mathbf{M}_4^{1,1} & \mathbf{M}_4^{1,2} & 0 & 0 \\ \mathbf{M}_4^{2,1} & \mathbf{M}_4^{2,2} & 0 & 0 \\ 0 & 0 & 0 & 0 \\ 0 & 0 & 0 & 0 \end{bmatrix} \tag{85}$$

$$\mathbf{M}_5 = \begin{bmatrix} \mathbf{M}_5^{1,1} & \mathbf{M}_5^{1,2} & 0 & \mathbf{M}_5^{1,4} \\ \mathbf{M}_5^{2,1} & \mathbf{M}_5^{2,2} & 0 & 0 \\ 0 & 0 & 0 & \mathbf{M}_5^{3,4} \\ \mathbf{M}_5^{4,1} & 0 & \mathbf{M}_5^{4,3} & \mathbf{M}_5^{4,4} \end{bmatrix} \tag{86}$$

where:

$$\mathbf{M}_1^{1,1} = \frac{4}{3} m_1 L_1^2 \tag{87}$$

$$\mathbf{M}_2^{1,1} = 4 m_2 L_1^2, \quad \mathbf{M}_2^{2,2} = \frac{4}{3} m_2 L_2^2 \tag{88}$$

$$\mathbf{M}_2^{1,2} = 2 L_1 L_2 m_2 \cos(\theta_1 - \theta_2) \tag{89}$$

$$\mathbf{M}_3^{1,1} = 4m_3L_1^2, \quad \mathbf{M}_3^{2,2} = 4m_3L_2^2 \tag{90}$$

$$\mathbf{M}_3^{3,3} = \frac{4}{3}m_3L_3^2, \quad \mathbf{M}_3^{1,2} = 4L_1L_2m_3\cos(\theta_1-\theta_2) \tag{91}$$

$$\mathbf{M}_3^{1,3} = 2L_1L_3m_3\cos(\theta_1-\theta_3) \tag{92}$$

$$\mathbf{M}_3^{2,3} = 2L_2L_3m_3\cos(\theta_2-\theta_3) \tag{93}$$

$$\mathbf{M}_4^{1,1} = 4m_4L_1^2 \tag{94}$$

$$\mathbf{M}_4^{2,2} = \frac{4}{3}m_4L_4^2 + 4m_4L_2^2 + 4m_4L_2L_4\cos(\beta) \tag{95}$$

$$\begin{aligned}\mathbf{M}_4^{1,2} = {} & 4L_1L_2m_4\cos(\theta_1-\theta_2) \\ & +2L_1L_4m_4\cos(\theta_1-\theta_2+\beta)\end{aligned} \tag{96}$$

$$\mathbf{M}_5^{1,1} = 4m_5L_1^2 \tag{97}$$

$$\mathbf{M}_5^{2,2} = 4m_5L_2^2 + 4m_5L_4^2 + 8m_5L_2L_4\cos(\beta) \tag{98}$$

$$\mathbf{M}_5^{4,4} = m_5 \tag{99}$$

$$\begin{aligned}\mathbf{M}_5^{1,2} = {} & 4L_1L_2m_5\cos(\theta_1-\theta_2) \\ & +4L_1L_4m_4\cos(\theta_1-\theta_2+\beta)\end{aligned} \tag{100}$$

$$\mathbf{M}_5^{1,4} = 2L_1m_5\cos(\theta_1) \tag{101}$$

$$\mathbf{M}_5^{3,4} = 2m_5L_2\cos(\theta_2) + 2m_5L_4\cos(\beta-\theta_2) \tag{102}$$

The total system generalized force vector $\mathbf{Q}_b$ is given by:

$$\mathbf{Q}_b = \mathbf{Q}_v + \mathbf{Q}_g + \mathbf{Q}_k + \mathbf{Q}_r + \mathbf{Q}_u \tag{103}$$

where $\mathbf{Q}_v$ is the total system inertia quadratic velocity vector, $\mathbf{Q}_g$ is the total system generalized force vector relative to the gravity forces, $\mathbf{Q}_k$ is the total system generalized force vector relative to the elastic force fields, $\mathbf{Q}_r$ is the total system generalized force vector relative to the dissipative force fields, and $\mathbf{Q}_u$ is the generalized force vector relative to the control action. In this equation, the following simplified structure of the generalized force vector associated with control action is assumed:

$$\mathbf{Q}_u = \begin{bmatrix} 0 \\ 0 \\ 0 \\ u \end{bmatrix} \tag{104}$$

where u represents the external control force provided by the active control system to be optimized. The total system inertia quadratic velocity vector $\mathbf{Q}_v$ can be computed as follows:

$$\mathbf{Q}_v = \mathbf{Q}_{v,1} + \mathbf{Q}_{v,2} + \mathbf{Q}_{v,3} + \mathbf{Q}_{v,4} + \mathbf{Q}_{v,5} \tag{105}$$

where $\mathbf{Q}_{v,1}$, $\mathbf{Q}_{v,2}$, $\mathbf{Q}_{v,3}$, $\mathbf{Q}_{v,4}$, and $\mathbf{Q}_{v,5}$ are the inertia quadratic velocity vectors of the rigid bodies that form the rigid mechanism which are respectively defined as:

$$\mathbf{Q}_{v,1} = \mathbf{0} \tag{106}$$

$$\mathbf{Q}_{v,2} = \begin{bmatrix} -2L_1L_2m_2\sin(\theta_1-\theta_2)\dot{\theta}_2^2 \\ \\ 2L_1L_2m_2\sin(\theta_1-\theta_2)\dot{\theta}_1^2 \\ \\ 0 \\ \\ 0 \end{bmatrix} \tag{107}$$

$$\mathbf{Q}_{v,3} = \begin{bmatrix} -4L_1L_2m_3\sin(\theta_1-\theta_2)\dot{\theta}_2^2 \\ -2L_1L_3m_3\sin(\theta_1-\theta_3)\dot{\theta}_3^2 \\ \\ 4L_1L_2m_3\sin(\theta_1-\theta_2)\dot{\theta}_1^2 \\ -2L_2L_3m_3\sin(\theta_2-\theta_3)\dot{\theta}_3^2 \\ \\ 2L_1L_3m_3\sin(\theta_1-\theta_3)\dot{\theta}_1^2 \\ +2L_2L_3m_3\sin(\theta_2-\theta_3)\dot{\theta}_2^2 \\ \\ 0 \end{bmatrix} \tag{108}$$

$$\mathbf{Q}_{v,4} = \begin{bmatrix} -4L_1L_2m_4\sin(\theta_1-\theta_2)\dot{\theta}_2^2 \\ -2L_1L_4m_4\sin(\theta_1-\theta_2+\beta)\dot{\theta}_2^2 \\ \\ 4L_1L_2m_4\sin(\theta_1-\theta_2)\dot{\theta}_1^2 \\ +2L_1L_4m_4\sin(\theta_1-\theta_2+\beta)\dot{\theta}_1^2 \\ \\ 0 \\ \\ 0 \end{bmatrix} \tag{109}$$

$$\mathbf{Q}_{v,5} = \begin{bmatrix} -4L_1L_2m_5\sin(\theta_1-\theta_2)\dot{\theta}_2^2 \\ -4L_1L_4m_5\sin(\theta_1-\theta_2+\beta)\dot{\theta}_2^2 \\ \\ 4L_1L_2m_5\sin(\theta_1-\theta_2)\dot{\theta}_1^2 \\ +4L_1L_4m_5\sin(\theta_1-\theta_2+\beta)\dot{\theta}_1^2 \\ \\ 0 \\ \\ 2L_1m_5\sin(\theta_1)\dot{\theta}_1^2 \\ -2L_4m_5\sin(\beta-\theta_2)\dot{\theta}_2^2 \\ +2L_2m_5\sin(\theta_2)\dot{\theta}_2^2 \end{bmatrix} \tag{110}$$

The total system generalized force vector relative to the gravity forces $\mathbf{Q}_g$ can be computed as follows:

$$\mathbf{Q}_g = \mathbf{Q}_{g,1} + \mathbf{Q}_{g,2} + \mathbf{Q}_{g,3} + \mathbf{Q}_{g,4} + \mathbf{Q}_{g,5} \tag{111}$$

where $\mathbf{Q}_{g,1}$, $\mathbf{Q}_{g,2}$, $\mathbf{Q}_{g,3}$, $\mathbf{Q}_{g,4}$, and $\mathbf{Q}_{g,5}$ are the generalized gravitational force vectors of the rigid bodies that form the rigid mechanism which are respectively defined as:

$$\mathbf{Q}_{g,1} = \begin{bmatrix} -m_1gL_1\cos(\theta_1) \\ 0 \\ 0 \\ 0 \end{bmatrix} \tag{112}$$

$$\mathbf{Q}_{g,2} = \begin{bmatrix} -2m_2gL_1\cos(\theta_1) \\ -m_2gL_2\cos(\theta_2) \\ 0 \\ 0 \end{bmatrix} \tag{113}$$

$$\mathbf{Q}_{g,3} = \begin{bmatrix} -2m_3gL_1\cos(\theta_1) \\ -2m_3gL_2\cos(\theta_2) \\ -m_3gL_3\cos(\theta_3) \\ 0 \end{bmatrix} \tag{114}$$

$$\mathbf{Q}_{g,4} = \begin{bmatrix} -2m_4gL_1\cos(\theta_1) \\ \\ -2m_4gL_2\cos(\theta_2) \\ -m_4gL_4\cos(\beta-\theta_2) \\ \\ 0 \\ \\ 0 \end{bmatrix} \tag{115}$$

$$\mathbf{Q}_{g,5} = \begin{bmatrix} -2m_5gL_1\cos(\theta_1) \\ \\ -2m_5gL_2\cos(\theta_2) \\ -2m_5gL_4\cos(\beta-\theta_2) \\ \\ 0 \\ \\ -m_5g \end{bmatrix} \tag{116}$$

The total system generalized force vector relative to the elastic force fields $\mathbf{Q}_k$ is given by:

$$\mathbf{Q}_k = \mathbf{Q}_{k,1} + \mathbf{Q}_{k,2} + \mathbf{Q}_{k,3} \tag{117}$$

where $\mathbf{Q}_{k,1}$, $\mathbf{Q}_{k,2}$, and $\mathbf{Q}_{k,3}$ are the generalized elastic force vectors of the elastic components that form the rigid mechanism which are respectively defined as:

$$\mathbf{Q}_{k,1} = \begin{bmatrix} (p_1 - k_1 f_{k,1})\, 2L_1\cos(\theta_1) \\ -k_1 g_{k,1} 2L_1\cos(\theta_1) \\ \\ (p_1 - k_1 f_{k,1})\, 2L_2\cos(\theta_2) \\ -k_1 g_{k,1} 2L_2\cos(\theta_2) \\ \\ (p_1 - k_1 f_{k,1})\,(L_3 + L_E)\cos(\theta_3) \\ -k_1 g_{k,1}\,(L_3 + L_E)\cos(\theta_3) \\ \\ 0 \end{bmatrix} \tag{118}$$

$$\mathbf{Q}_{k,2} = \begin{bmatrix} 0 \\ 0 \\ 0 \\ -k_2 x \end{bmatrix} \tag{119}$$

$$\mathbf{Q}_{k,3} = \begin{bmatrix} k_3\,(f_{k,3} + g_{k,3})\, 2L_1\cos(\theta_1) \\ +k_3\,(h_{k,3} + l_{k,3})\, 2L_1\cos(\theta_1) \\ \\ k_3\,(f_{k,3} + g_{k,3})\, 2\,(L_4\cos(\beta-\theta_2)) \\ +k_3\,(h_{k,3} + l_{k,3})\, 2\,(L_4\cos(\beta-\theta_2)) \\ +k_3\,(f_{k,3} + g_{k,3})\, 2\,(L_2\cos(\theta_2)) \\ +k_3\,(h_{k,3} + l_{k,3})\, 2\,(L_2\cos(\theta_2)) \\ \\ k_3\,(f_{k,3} + g_{k,3}) \\ +k_3\,(h_{k,3} + l_{k,3}) \end{bmatrix} \tag{120}$$

where:

$$f_{k,1} = 2L_1\sin(\theta_1) + 2L_2\sin(\theta_2) \tag{121}$$

$$g_{k,1} = (L_3 + L_E)\sin(\theta_3) - H_E \tag{122}$$

$$f_{k,3} = H_0 + s, \quad g_{k,3} = -2L_1\sin(\theta_1) \tag{123}$$

$$h_{k,3} = 2L_4\sin(\beta-\theta_2), \quad l_{k,3} = -2L_2\sin(\theta_2) - x \tag{124}$$

The total system generalized force vector relative to the dissipative force fields $\mathbf{Q}_r$ is given by:

$$\mathbf{Q}_r = \mathbf{Q}_{r,1} + \mathbf{Q}_{r,2} + \mathbf{Q}_{r,3} \tag{125}$$

where $\mathbf{Q}_{r,1}$, $\mathbf{Q}_{r,2}$, and $\mathbf{Q}_{r,3}$ are the generalized damping force vectors of the damping components that form the rigid mechanism which are respectively defined as:

$$\mathbf{Q}_{r,1} = \begin{bmatrix} -r_1\,(f_{r,1} + g_{r,1})\, 2L_1\cos(\theta_1) \\ -r_1 h_{r,1} 2L_1\cos(\theta_1) \\ \\ -r_1\,(f_{r,1} + g_{r,1})\, 2L_2\cos(\theta_2) \\ -r_1 h_{r,1} 2L_2\cos(\theta_2) \\ \\ -r_1\,(f_{r,1} + g_{r,1})\,(L_3 + L_E)\cos(\theta_3) \\ -r_1 h_{r,1}\,(L_3 + L_E)\cos(\theta_3) \\ \\ 0 \end{bmatrix} \tag{126}$$

$$\mathbf{Q}_{r,2} = \begin{bmatrix} 0 \\ 0 \\ 0 \\ -r_2\dot{x} \end{bmatrix} \tag{127}$$

$$\mathbf{Q}_{r,3} = \begin{bmatrix} r_3\,(f_{r,3} + g_{r,3} + h_{r,3})\, 2L_1\cos(\theta_1) \\ \\ r_3\,(f_{r,3} + g_{r,3} + h_{r,3})\, l_{r,3} \\ \\ 0 \\ \\ r_3\,(f_{r,3} + g_{r,3} + h_{r,3}) \end{bmatrix} \tag{128}$$

where:

$$f_{r,1} = 2L_1\cos(\theta_1)\dot{\theta}_1, \quad g_{r,1} = 2L_2\cos(\theta_2)\dot{\theta}_2 \tag{129}$$

$$h_{r,1} = (L_3 + L_E)\cos(\theta_3)\dot{\theta}_3 \tag{130}$$

$$f_{r,3} = \dot{s} - 2L_1\cos(\theta_1)\dot{\theta}_1 \tag{131}$$

$$g_{r,3} = -2L_4\cos(\beta-\theta_2)\dot{\theta}_2 \tag{132}$$

$$h_{r,3} = -2L_2\cos(\theta_2)\dot{\theta}_2 - \dot{x} \tag{133}$$

$$l_{r,3} = 2\,(L_4\cos(\beta-\theta_2) + L_2\cos(\theta_2)) \tag{134}$$

The dynamic equations reported in this subsection completely describe the total system mass matrix $\mathbf{M}$ and the total system generalized force vector $\mathbf{Q}_b$ of the pantograph mechanism considered as the case study of the paper.

B. Constrained Dynamic Equations of the Pantograph Mechanism

In this subsection, the closed-loop kinematic structure of the pantograph mechanism is described considering an appropriate set of algebraic constraint equations. The pantograph system forms a closed-chain mechanism which can be modeled considering the following closure equations which form the constraint vector denoted with $\mathbf{C}$ and given by:

$$\mathbf{C} = \begin{bmatrix} 2L_1\cos(\theta_1) + 2L_2\cos(\theta_2) \\ +2L_3\cos(\theta_3) - H_1 \\ \\ 2L_1\sin(\theta_1) + 2L_2\sin(\theta_2) \\ +2L_3\sin(\theta_3) - H_2 \end{bmatrix} \tag{135}$$

where H_1 and H_2 are constant geometric parameters associated with the dimension of the closed-chain mechanism shown in Figure 7. The constraint Jacobian matrix $\mathbf{C_q}$ and the constraint quadratic velocity vector $\mathbf{Q}_d$ associated with the closure equations are respectively given by:

$$\mathbf{C_q} = \begin{bmatrix} -2L_1\sin(\theta_1) & 2L_1\cos(\theta_1) \\ -2L_2\sin(\theta_2) & 2L_2\cos(\theta_2) \\ -2L_3\sin(\theta_3) & 2L_3\cos(\theta_3) \\ 0 & 0 \end{bmatrix}^T \tag{136}$$

and

$$\mathbf{Q}_d = \begin{bmatrix} 2L_1\cos(\theta_1)\dot{\theta}_1^2 + 2L_2\cos(\theta_2)\dot{\theta}_2^2 \\ +2L_3\cos(\theta_3)\dot{\theta}_3^2 \\ \\ 2L_1\sin(\theta_1)\dot{\theta}_1^2 + 2L_2\sin(\theta_2)\dot{\theta}_2^2 \\ +2L_3\sin(\theta_3)\dot{\theta}_3^2 \end{bmatrix} \tag{137}$$

Considering the closure equations used for modeling the closed-chain topology of the pantograph mechanism and assuming a standard assembly procedure for the dynamic equations, one obtains the following set of differential-algebraic equations:

$$\begin{cases} \mathbf{M}\ddot{\mathbf{q}} = \mathbf{Q}_b - \mathbf{C}_\mathbf{q}^T\lambda \\ \\ \mathbf{C_q}\ddot{\mathbf{q}} = \mathbf{Q}_d \end{cases} \tag{138}$$

Employing a computational approach based on the augmented formulation, the nonlinear equations of motion of the mechanical system under consideration can be numerically solved by using a standard integration scheme combined with a numerical procedure for the stabilization of the constraint drift.

C. Dynamic Analysis and Control Design of the Pantograph Mechanism

In this subsection, the dynamic analysis of the pantograph mechanism is described and the numerical results found implementing the nonlinear time law for the control actuator are discussed. Once that a reliable nonlinear dynamic model for the pantograph mechanism is obtained, one can use the mechanical model for performing numerical experiments by means of dynamical simulations based on the use of effective solution algorithms suitable for analyzing multibody systems [61], [62]. The numerical scheme used to achieve this goal is the well-established fourth-order explicit Runge-Kutta algorithm because of its superior performance compared with the first-order forward Euler method. The Runge-Kutta method is also convenient to use in the numerical solution of the adjoint equations. In particular, in this study, an active control action is collocated between the pan-head and the pantograph superior arm. The optimal time law for the control actuator is designed to diminish the variation of the force arising from the interaction between the pantograph mechanism and the catenary cable. For this purpose, it is of great importance to not affect the average value of the interaction force. The actuated device is used also for reducing the oscillations of the pantograph arms. The input law for the controller is designed considering an open-loop control action, which can be optimized by using the adjoint approach described in the manuscript. By doing so, the cost function designed for regulating the dynamic behavior of the mechanism iteratively achieves the convergence as represented in Figure 8(a). The final time law for the control action corresponding to the converged cost function is shown in Figure 8(b). Figure 9(a)

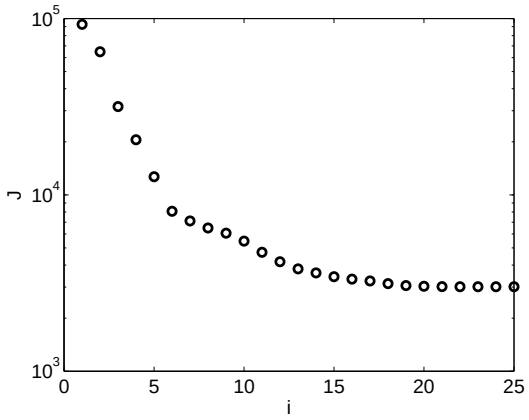

(a) Convergence of the cost function.

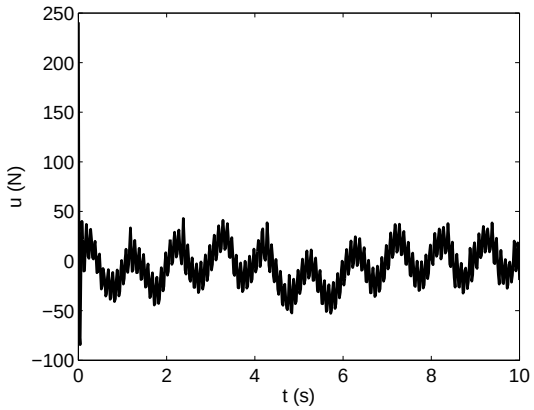

(b) Optimal control force.

Fig. 8. Optimization of the control law.

shows the time evolution of the interaction force without the presence of the control action, while Figure 9(b) represents the contact force when the open-loop control action is applied on the pantograph mechanism. When there is no control action, the pan-head displacement and velocity are respectively represented in Figures 10(a) and 11(a). The time evolution of the same variables are respectively shown in Figures 10(b) and 11(b) considering the application of the nonlinear controller developed in this work. Observing Figures 9(a) and 9(b), one can deduce that the open-loop controller induces

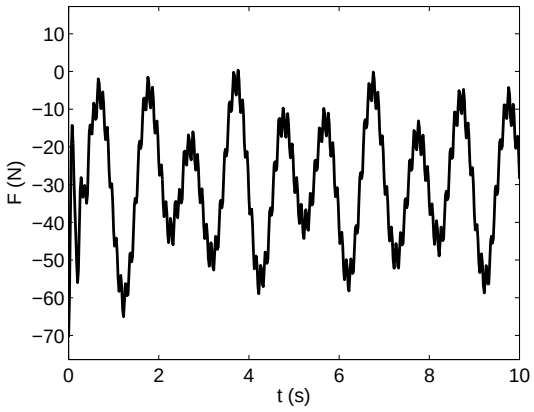

(a) Contact force without the optimal control action.

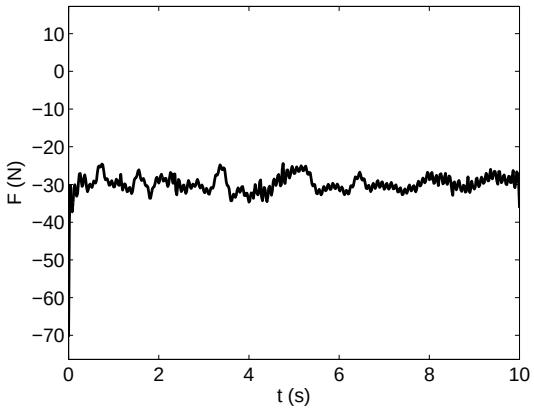

(b) Contact force with the optimal control action.

Fig. 9. Interaction force.

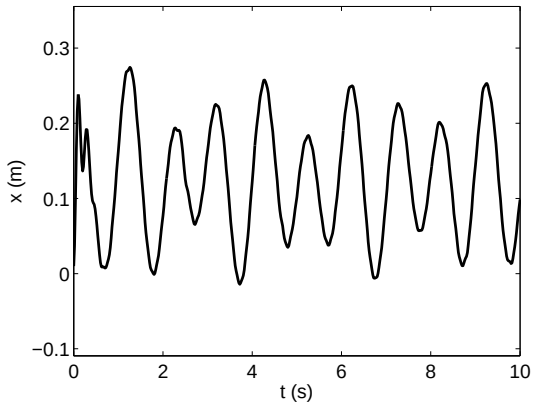

(a) Uncontrolled motion.

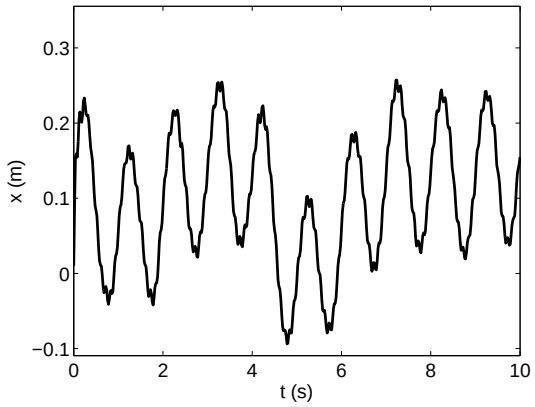

(b) Controlled motion.

Fig. 10. Pan-head displacement.

a considerable attenuation of the interaction force deriving from the coupling between pantograph mechanism and the catenary cable. An excessively strong contact force can be detrimental for the contact surfaces and for the structural integrity of the catenary wire, while a too weak contact force can lead to the separation between the pantograph mechanism and the suspended line, thereby damaging the coupling mechanism because of the starting of the electrical arcing. Keeping an optimal value of the magnitude of the contact force is, therefore, absolutely necessary for the proper system functioning. The improvement in the quality of the contact obtained by using the methodology described in this section is quantified employing the numerical parameters reported in Table III. Furthermore, a close observation of Figures 10(a), 10(b), 11(a), and 11(b) reveals that the application of the nonlinear control action devised for the planar pantograph mechanism does not alter the normal functioning of the pantograph pan-head and, therefore, an effective contact is still guaranteed. Thus, the numerical results reported in this section clearly demonstrates the effectiveness of the computational approach developed in the paper for improving the contact quality of the current collection system based on the pantograph mechanism and the suspended electrical line.

TABLE III
CONTACT PARAMETERS.

Contact Force	Mean	Standard Deviation
Uncontrolled Motion	$-29.570(\mathrm{N})$	$15.602(\mathrm{N})$
Controlled Motion	$-29.876(\mathrm{N})$	$2.798(\mathrm{N})$
Percentage Reduction	$1.036(\%)$	$82.064(\%)$

V. SUMMARY AND CONCLUSIONS

The authors' academic focus encompasses wide research areas closely related to practical problems in the field of mechanical engineering. Thus, the principal disciplines of interest for the authors are multibody system dynamics, nonlinear optimal control, and applied system identification. Multibody dynamics is concentrated on the dynamic analysis of articulated mechanisms and complex machines composed of rigid and flexible components constrained by kinematic pairs [63]–[66]. Nonlinear control is concerned with the study of effective algorithms which allow for controlling mechanical systems described by nonlinear dynamical models [67]–[70]. System Identification is based on the study of numerical methods suitable for obtaining dynamical models of mechanical systems using experimental data based on sensor measurements [71]–[74]. The theoretical and practical connections between these three disciplines are, therefore, apparent [75]. This work, on the other hand, deals with the dynamics and control of a closed-loop kinematically-driven mechanism used for predicting the evolution in time of the pantograph/catenary contact force considering the multibody system approach.

In this study, a recursive Lagrangian approach is used for deriving a two-dimensional dynamical model of a kinematically-driven double inverted pendulum system as

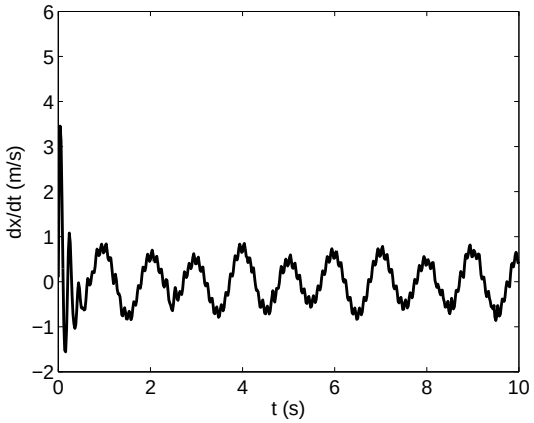

(a) Uncontrolled motion.

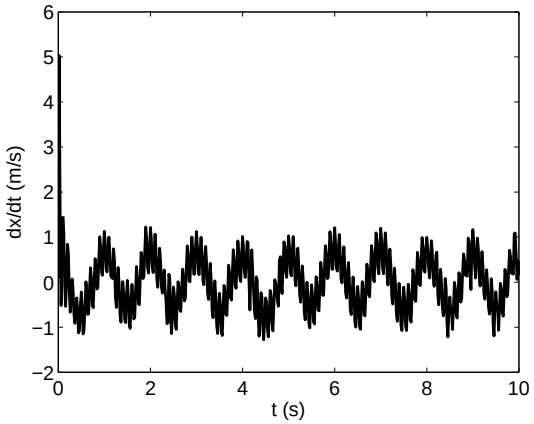

(b) Controlled motion.

Fig. 11. Pan-head velocity.

well as of the pantograph mechanism. The resulting mechanical models are based on the analytical techniques of multibody system dynamics and are employed for carrying out dynamical simulations. In particular, while the double inverted pendulum system is used as a demonstrative example of the analytical approach developed in the paper for modeling kinematically-driven multibody mechanical systems, the main objective of the case study is to obtain an appropriate control law for the force actuator interposed between the superior arm and the pan-head of the pantograph mechanism. If the control system is properly tuned, the interaction of the pantograph with the suspended line can be significantly improved. First, the nonlinear algebraic constraint equations, which represent the closed-chain geometry of the four-bar mechanism used for modeling the pantograph as a multibody system, are imposed by employing a Lagrangian approach. Subsequently, the design of a nonlinear control action aimed at reducing the contact force applied on the multibody mechanism is performed in this investigation by solving a nonlinear control problem considering an iterative algorithm that makes use of the adjoint method. The dynamic analysis carried out in this paper demonstrates the effectiveness of the nonlinear control action designed for the multibody system used for modeling the pantograph/catenary mechanism.

This investigation is focused on the design of a nonlinear control law suitable for controlling the interaction force produced by the contact between the sliding strips of the pantograph and the suspended line that provides the electrical energy to the train. To this end, the development of a detailed mechanical model of the closed-loop mechanism that models the dynamics of the multibody system at hand represents the first fundamental step for the subsequent design of effective control laws. The control law is necessary for controlling the force actuator properly designed to regulate the interaction with the suspended line. A twofold purpose is considered to this end, namely to reduce the oscillations of the closed-loop mechanism and to attenuate the contact force. An augmented set of Lagrangian coordinates and a recursive formulation approach are employed for the explicit derivation of the equations of motion of the system under consideration in this investigation. The multibody model developed in this paper is based on simplifying assumptions for the layout of the pantograph mechanism. The basic articulations of the rigid frames of this mechanical system are schematized as a planar four-bar linkage composed only of rigid bodies. The pneumatic actuator that provides the lift force for the pantograph mechanism is schematized considering an external force field having a nonlinear structure using a lumped parameter approach. Furthermore, the pantograph suspension mechanism is modeled considering a linear elastic element in parallel with a linear damping element. A simplifying assumption was used in order to take into account the interaction force between the contact mechanism and the suspended line. This force is modeled considering a simple elastic element interposed between a kinematically driven element and the pan-head of the pantograph mechanism. The motion law assigned to the kinematically driven element takes into account the dynamic effects of the catenary cable on the pantograph mechanism. Employing the analytical and computational approach described in the paper, the resulting numerical simulations confirmed the physical consistency of the dynamic behavior obtained for the multibody mechanical system of interest for this study.

In this work, a nonlinear feedforward controller is developed for a closed-chain pantograph/catenary multibody model. The goal of the control law designed for this mechanical system is to decrease the attrition of the pantograph strips and to suppress the mechanical oscillations of the closed-loop mechanism that forms the pantograph. To this end, an appropriate cost function is designed for transforming the nonlinear control problem analyzed in this paper into a nonlinear optimization problem. The cost function associated with the performance of the optimal controller is devised in such a way that the variation of the interaction force between the strips of the pantograph and the catenary cable of the suspended line is diminished without affecting its average value. Furthermore, the nonlinear control law assigned to the force actuator interposed between the contact elements is designed by using an iterative algorithm deriving from the combination of the optimal control theory and the adjoint numerical analysis. The optimization method mentioned before is widely used in computational fluid dynamics and has been recently adopted in the field of applied mechanics. The final result of the adjoint numerical algorithm is an explicit time function for the control force that reflects the desired dynamic behavior by minimizing a performance index that serves as a quantitative metric for the performance of the control law. By doing so, significant improvements can be obtained for the interaction between the contact strips of

the pantograph and the cable of the suspended line, as demonstrated by the numerical results presented in the paper. When compared with the dynamic behavior of the multibody mechanical system considered in this work without the presence of any controller, the optimal time law computed for the feedforward controller devised in this investigation leads to a large reduction of the variation of the interaction force that characterizes the contact. Therefore, the methodology proposed in this investigation represents a viable solution for improving the contact between the pantograph mechanism and the catenary cable.

Authors' Contributions

This research paper was principally developed by the first author (Carmine Maria Pappalardo). The detailed review carried out by the second author (Domenico Guida) considerably improved the quality of the work.

References

[1] F. Villecco, "On the Evaluation of Errors in the Virtual Design of Mechanical Systems," *Machines*, vol. 6, no.3, 36, 2018.

[2] P. Sena, P. Attianese, M. Pappalardo, and F. Villecco, "FIDELITY: Fuzzy Inferential Diagnostic Engine for on-LIne supporT to phYsicians," Proceedings of the 4th International Conference on the Development of Biomedical Engineering, Ho Chi Minh City, Vietnam, 8-10 January 2012, IFMBE Proceedings, Springer Verlag: Berlin, Germany, pp396-400, 2013.

[3] M. Ghomshei, F. Villecco, S. Porkhial, and M. Pappalardo, "Complexity in Energy Policy: A Fuzzy Logic Methodology," Proceedings of the 6th International Conference on Fuzzy Systems and Knowledge Discovery, Tianjin, China, 14-16 August 2009, IEEE, Los Alamitos, CA, USA, vol. 7, pp128-131, 2009.

[4] Y. Zhai, L. Liu, W. Lu, Y. Li, S. Yang, and F. Villecco, "The Application of Disturbance Observer to Propulsion Control of Submini Underwater Robot," Proceedings of the ICCSA 2010 International Conference on Computational Science and Its Applications, Fukuoka, Japan, 23-26 March 2010, Lecture Notes in Computer Science, Springer: Berlin, Germany, pp590-598, 2010.

[5] P. Sena, M. D'Amore, M. Pappalardo, A. Pellegrino, A. Fiorentino, and F. Villecco, "Studying the Influence of Cognitive Load on Driver's Performances by a Fuzzy Analysis of Lane Keeping in a Drive Simulation," IFAC Proc. 2013, vol. 46, no.21, pp151-156, 2013.

[6] M. Ghomshei, and F. Villecco, "Energy Metrics and Sustainability," Proceedings of the International Conference on Computational Science and Its Applications, Seoul, Korea, 29 June - 2 July 2009, Lecture Notes in Computer Science, Springer Verlag, Berlin, Germany, pp693-698, 2009.

[7] P. Sena, P. Attianese, F. Carbone, A. Pellegrino, A. Pinto, and F. Villecco, "A Fuzzy Model to Interpret Data of Drive Performances from Patients with Sleep Deprivation," *Computational and mathematical methods in medicine*, 868410, 2012.

[8] Y. Zhang, Z. Li, J. Gao, J. Hong, F. Villecco, and Y. Li, "A method for designing assembly tolerance networks of mechanical assemblies," *Mathematical Problems in Engineering*, 513958, 2012.

[9] F. Villecco, and A. Pellegrino, "Evaluation of Uncertainties in the Design Process of Complex Mechanical Systems," *Entropy*, vol. 19, no.9, 475, 2017.

[10] A. Formato, D. Ianniello, F. Villecco, T. L. L. Lenza, and D. Guida, "Design Optimization of the Plough Working Surface by Computerized Mathematical Model," *Emirates Journal of Food and Agriculture*, vol. 29, no.1, pp36-44, 2017.

[11] A. Pellegrino, and F. Villecco, "Design Optimization of a Natural Gas Substation with Intensification of the Energy Cycle," *Mathematical Problems in Engineering*, 294102, 2010.

[12] A. Formato, D. Guida, D. Ianniello, F. Villecco, T. L. L. Lenza, and A. Pellegrino, "Design of Delivery Valve for Hydraulic Pumps," *Machines*, vol. 6, no.4, 44, 2018.

[13] G. Poetsch, J. Evans, R. Meisinger, W. Kortum, W. Baldauf, A. Veitl, and J. Wallaschek, "Pantograph/Catenary Dynamics and Control," *Journal of Vehicle System Dynamics*, vol. 28, no.2-3 pp159-195, 1997.

[14] J. Ambrosio, J. Pombo, and M. Pereira, "Optimization of High-Speed Railway Pantographs for Improving Pantograph-Catenary Contact," *Theoretical and Applied Mechanics Letters*, vol. 3, no.1, 013006, 2013.

[15] J. Ambrosio, J. Pombo, M. Pereira, P. Antunes, and A. Mosca, "Computational Procedure for the Dynamic Analysis of the Catenary-Pantograph Interaction in High-Speed Trains," *Journal of Theoretical and Applied Mechanics*, vol. 50, no.3, pp681-699, 2012.

[16] C. Wei, "Stabilisation by Stochastic Feedback Control Based on Discrete-time Observations," *IAENG International Journal of Applied Mathematics*, vol. 49, no.4, pp488-494, 2019.

[17] L. Chen, and J. Sun, J. "Distributed Optimal Control for Multi-agent Systems with Impulsive Effects," *IAENG International Journal of Applied Mathematics*, vol. 49, no.1, pp86-89, 2019.

[18] A. Maarif, A. I. Cahyadi, S. Herdjunanto, Iswanto, and Y. Yamamoto, "Tracking Control of Higher Order Reference Signal Using Integrators and State Feedback," *IAENG International Journal of Computer Science*, vol. 46, no.2, pp208-216, 2019.

[19] L. Wang, "Dynamics of an Almost Periodic Single-Species System with Harvesting Rate and Feedback Control on Time Scales," *IAENG International Journal of Computer Science*, vol. 46, no.2, pp237-242, 2019.

[20] G. Chen, X. Yi, Z. Zhang, and S. Qiu, "Solving Optimal Power Flow using Cuckoo Search Algorithm with Feedback Control and Local Search Mechanism," *IAENG International Journal of Computer Science*, vol. 46, no.2, pp321-331, 2019.

[21] M. A. Jami'in and E. Julianto, "Hierarchical Algorithms of Quasi-Linear ARX Neural Networks for Identification of Nonlinear Systems," *Engineering Letters*, vol. 25, no.3, pp321-328, 2017.

[22] J. Zhang, L. Yu, and L. Ding, "Velocity Feedback Control of Swing Phase for 2-DoF Robotic Leg Driven by Electro-hydraulic Servo System," *Engineering Letters*, vol. 24, no.4, pp378-383, 2016.

[23] Q. W. Guo, W. D. Song, M. Gao, and D. Fang, "Advanced Guidance Law Design for Trajectory-Corrected Rockets with Canards under Single Channel Control," *Engineering Letters*, vol. 24, no.4, pp469-477, 2016.

[24] H. Liu and Y. Li, "Safety Evaluation of a Long-Span Steel Trestle with an Extended Service Term Age in a Coastal Port Based on Identification of Modal Parameters," *Engineering Letters*, vol. 24, no.1, pp84-92, 2016.

[25] I. I. Lazaro, A. Alvarez, and J. Anzurez, "The Identification Problem Applied to Periodic Systems Using Hartley Series," *Engineering Letters*, vol. 21, no.1, pp36-43, 2013.

[26] C. Lv, F. Yu, M. Zhu, and S. Xiao, "AUV Real-time Dynamic Obstacle Avoidance Strategy Based on Relative Motion," *Engineering Letters*, vol. 27, no.1, pp234-240, 2019.

[27] L. Wang, "Dynamic Output Feedback Guaranteed Cost Control for Linear Nominal Impulsive Systems," *Engineering Letters*, vol. 26, no.4, pp405-409, 2018.

[28] T. K. Tanev, A. Cammarata, D. Marano, and R. Sinatra, "Elastostatic model of a new hybrid minimally-invasive-surgery robot," The 14th IFToMM World Congress, Taipei, Taiwan, October, 2015.

[29] A. Cammarata, "A novel method to determine position and orientation errors in clearance-affected overconstrained mechanisms," *Mechanism and Machine Theory*, vol. 118, pp247-264, 2017.

[30] A. Cammarata, I. Calió, A. Greco, M. Lacagnina, and G. Fichera, "Dynamic stiffness model of spherical parallel robots," *Journal of Sound and Vibration*, vol. 384, pp312-324, 2016.

[31] M. Callegari, A. Cammarata, A. Gabrielli, and R. Sinatra, "Kinematics and dynamics of a 3-CRU spherical parallel robot," ASME 2007 International Design Engineering Technical Conferences and Computers and Information in Engineering Conference, American Society of Mechanical Engineers, pp933-941, 2007.

[32] M. Y. Karelina, E. Krylov, C. Rossi, S. Savino, and F. Timpone, "A Multibody Model of Federica Hand," *Engineering Letters*, vol. 24, no.4, pp406-417, 2016.

[33] F. Renno, S. Strano, and M. Terzo, "Development and Validation of an Air Spring Multiphysical Model," *Engineering Letters*, vol. 25, no.2, pp176-182, 2017.

[34] D. Vlasenko and R. Kasper, "Generation of equations of motion in reference frame formulation for fem models," *Engineering Letters*, vol. 16, no.4, pp537-544, 2008.

[35] F. E. Udwadia, and R. E. Kalaba, "A New Perspective on Constrained Motion," *Proceedings of the Royal Society of London, Series A: Mathematical and Physical Sciences*, vol. 439, no.1906, pp407-410, 1992.

[36] Y. Song, Z. Liu, H. Ouyang, H. Wang, and X. Lu, "Sliding mode control with PD sliding surface for high-speed railway pantograph-catenary contact force under strong stochastic wind field," *Shock and Vibration*, vol. 2017, 2017.

[37] Y. Song, H. Ouyang, Z. Liu, G. Mei, H. Wang, and X. Lu, "Active control of contact force for high-speed railway pantograph-catenary based on multi-body pantograph model," *Mechanism and Machine Theory*, vol. 115, pp35-59, 2017.

[38] M. T. Ko, M. Yokoyama, Y. Yamashita, S. Kobayashi, and T. Usuda, "Contact force control of an active pantograph for high speed trains," *Journal of Physics: Conference Series*, vol. 744, no.1, 012151, 2016.

[39] L. Zhang, J. Zhang, T. Li, and W. Zhang, "Influence of pantograph fixing position on aerodynamic characteristics of high-speed trains," *Journal of Modern Transportation*, vol. 25, no.1, pp34-39, 2017.

[40] R. Li, W. Zhang, Z. Ning, B. Liu, D. Zou, and W. Liu, "Influence of a high-speed train passing through a tunnel on pantograph aerodynamics and pantograph-catenary interaction," *Proceedings of the Institution of Mechanical Engineers, Part F: Journal of Rail and Rapid Transit*, vol. 231, no.2, pp198-210, 2017.

[41] P. Navik, A. Ronnquist, and S. Stichel, "A wireless railway catenary structural monitoring system: Full-scale case study," *Case Studies in Structural Engineering*, vol. 6, pp22-30, 2016.

[42] P. Navik, A. Ronnquist, and S. Stichel, "Identification of system damping in railway catenary wire systems from full-scale measurements," *Engineering Structures*, vol. 113, pp71-78, 2016.

[43] A. Schirrer, G. Aschauer, E. Talic, M. Kozek, and S. Jakubek, "Catenary emulation for hardware-in-the-loop pantograph testing with a model predictive energy-conserving control algorithm," *Mechatronics*, vol. 41, pp17-28, 2017.

[44] A. Schirrer, G. Aschauer, and S. Jakubek, "Hardware-in-the-Loop Testing of High-Speed Pantographs Using Real-Time Catenary Emulation," *Dynamics and Control of Advanced Structures and Machines, Springer, Cham.*, pp75-83, 2017.

[45] W. H. Zhang, G. M. Mei, X. J. Wu, Z. Shen, "Hybrid simulation of dynamics for the pantograph-catenary system," *Vehicle System Dynamics*, vol. 38, no.6, pp393-414, 2002.

[46] W. H. Zhang, G. M. Mei, X. J. Wu, L. Q. Chen, "A study on dynamic behaviour of pantographs by using hybrid simulation method," *Proceedings of the Institution of Mechanical Engineers, Part F: Journal of Rail and Rapid Transit*, vol. 219, no.3, pp189-199, 2005.

[47] S. Daocharoenporn, M. Mongkolwongrojn, K. Kulkarni, and A. A. Shabana, "Prediction of the Pantograph/Catenary Wear Using Nonlinear Multibody System Dynamic Algorithms," *Journal of Tribology*, vol. 141, no.5, 051603, 2019.

[48] X. Lu, H. Zhang, Z. Liu, F. Duan, Y. Song, and H. Wang, "Estimator-based H-infinite control considering actuator time delay for active double-pantograph in high-speed railways," *Journal of Low Frequency Noise, Vibration and Active Control*, 1461348419876791, 2019.

[49] F. Vesali, H. Molatefi, M. A. Rezvani, B. Moaveni, and M. Hecht, "New control approaches to improve contact quality in the conventional spans and overlap section in a high-speed catenary system," *Proceedings of the Institution of Mechanical Engineers, Part F: Journal of Rail and Rapid Transit*, 0954409718822861, 2019.

[50] P. Zdziebko, A. Martowicz, and T. Uhl, "An investigation on the active control strategy for a high-speed pantograph using co-simulations," *Proceedings of the Institution of Mechanical Engineers, Part I: Journal of Systems and Control Engineering*, vol. 233, no.4, pp370-383, 2019.

[51] S. Kulkarni, C. M. Pappalardo, and A. A. Shabana, "Pantograph/catenary contact formulations," *Journal of Vibration and Acoustics*, vol. 139, no. 1, 011010, 2017.

[52] C. M. Pappalardo, P. D. Patel, B. Tinsley, A. A, Shabana, "Contact force control in multibody pantograph/catenary systems," *Proceedings of the Institution of Mechanical Engineers, Part K: Journal of Multibody Dynamics*, vol. 230, no.4, pp307-328, 2016.

[53] A. A. Shabana, *Dynamics of Multibody Systems*, Cambridge University Press: New York, NY, USA, 2013.

[54] A. Schutte, and F. Udwadia, "New Approach to the Modeling of Complex Multibody Dynamical Systems," *Journal of Applied Mechanics*, vol. 78, no.2, 021018, 2011.

[55] F. Marques, A. P. Souto, and P. Flores, "On the Constraints Violation in Forward Dynamics of Multibody Systems," *Multibody System Dynamics*, vol. 39, no.4, pp385-419, 2017.

[56] A. A. Shabana, *Computational Dynamics*, John Wiley and Sons: The Atrium, Southern Gate, Chichester, West Sussex, UK, 2009.

[57] J. G. Garcia De Jalon, and E. Bayo, *Kinematic and Dynamic Simulation of Multibody Systems: The Real-time Challenge*, Springer-Verlag: New York, NY, USA, 2012.

[58] K. Nachbagauer, S. Oberpeilsteiner, K. Sherif, and W. Steiner, "The Use of the Adjoint Method for Solving Typical Optimization Problems in Multibody Dynamics," *Journal of Computational and Nonlinear Dynamics*, vol. 10, no.6, 061011, 2015.

[59] S. Oberpeilsteiner, T. Lauss, K. Nachbagauer, and W. Steiner, "Optimal Input Design for Multibody Systems by using an Extended Adjoint Approach," *Multibody System Dynamics*, vol. 40, no.1, pp43-54, 2017.

[60] W. H. Press, S. A. Teukolsky, W. T. Vetterling, and B. P. Flannery, *Numerical Recipes 3rd Edition: The Art of Scientific Computing*, Cambridge University Press, 2007.

[61] K. T. Wehage, R. A. Wehage, B. Ravani, "Generalized Coordinate Partitioning for Complex Mechanisms based on Kinematic Substructuring," *Mechanism and Machine Theory*, vol. 92, pp464-483, 2015.

[62] G. Orzechowski, and J. Fraczek, "Integration of the Equations of Motion of Multibody Systems using Absolute Nodal Coordinate Formulation," *Acta Mechanica et Automatica*, vol. 6, no.2, pp75-83, 2012.

[63] M. C. De Simone, Z. B. Rivera, and D. Guida, "Obstacle Avoidance System for Unmanned Ground Vehicles by using Ultrasonic Sensors," *Machines*, vol. 6, no.2, 18, 2018.

[64] M. C. De Simone, S. Russo, Z. B. Rivera, and D. Guida, "Multibody Model of a UAV in Presence of Wind Fields," Proceedings - 2017 International Conference on Control, Artificial Intelligence, Robotics and Optimization, ICCAIRO 2017, 2018-January, pp83-88, 2018.

[65] M. C. De Simone and D. Guida, "Identification and control of a Unmanned Ground Vehicle by using Arduino," *UPB Scientific Bulletin, Series D: Mechanical Engineering*, vol. 80, no.1, pp141-154, 2018.

[66] M. C. De Simone and D. Guida, "On the Development of a Low Cost Device for Retrofitting Tracked Vehicles for Autonomous Navigation," Proceedings of the XXIII Conference of the Italian Association of Theoretical and Applied Mechanics (AIMETA 2017), 4-7 Spetember 2017, Salerno, Italy, 2017.

[67] C. M. Pappalardo and D. Guida, "Development of a New Inertial-based Vibration Absorber for the Active Vibration Control of Flexible Structures," *Engineering Letters*, vol. 26, no.3, pp372-385, 2018.

[68] M. C. De Simone, and D. Guida, "Control design for an under-actuated UAV model," *FME Transactions*, vol. 46, no.4, pp443-452, 2018.

[69] M. C. De Simone, and D. Guida, "Modal coupling in presence of dry friction," *Machines*, vol. 6, no.1, 8, 2018.

[70] M. C. De Simone, Z. B. Rivera, and D. Guida, "Finite element analysis on squeal-noise in railway applications," *FME Transactions*, vol. 46, no.1, pp93-100, 2018.

[71] C. M. Pappalardo and D. Guida, "System Identification and Experimental Modal Analysis of a Frame Structure," *Engineering Letters*, vol. 26, no.1, pp56-68, 2018.

[72] A. Concilio, M. C. De Simone, Z. B. Rivera, and D. Guida, "A new semi-active suspension system for racing vehicles," *FME Transactions*, vol. 45, no.4, pp578-584, 2017.

[73] M. C. De Simone, and D. Guida, "Dry Friction Influence on Structure Dynamics," COMPDYN 2015 - 5th ECCOMAS Thematic Conference on Computational Methods in Structural Dynamics and Earthquake Engineering, pp4483-4491, 2015.

[74] A. Quatrano, M. C. De Simone, Z. B. Rivera, and D. Guida, "Development and Implementation of a Control System for a Retrofitted CNC Machine by Using Arduino," *FME Transactions*, vol. 45, no.4, pp578-584, 2017.

[75] C. M. Pappalardo, and D. Guida, "On the Computational Methods for the Dynamic Analysis of Rigid Multibody Mechanical Systems," *Machines*, vol. 6, no.20, 2018.